Université de Montréal

The Consequences of CCL23/CCR1 Axis Signaling in KMT2A-MLLT3 Acute Myeloid Leukemia

By

Shahem Merjaneh

Molecular Biology Department

Faculty of Medicine

Thesis presented to obtain a degree of Master of Science (M.Sc.)

in Molecular Biology, option Systems Biology.

August 2020

Résumé

La leucémie myéloïde aiguë (LMA) est causée par une prolifération anormale de cellules souches sanguines immatures. Notre laboratoire se concentre sur un sous-groupe de la LMA représentant près de 30% de la LAM pédiatrique et caractérisé par la translocation chromosomique KMT2A-MLLT3. L'analyse par séquençage de l'ARN (RNA-seq) dans notre modèle de LMA médiée par la fusion KMT2A-MLLT3 et des échantillons de patients leucémiques a révélé que les gènes codant la chimiokine CCL23 et son récepteur correspondant CCR1 sont surexprimés dans cette maladie. Bien qu'il ait été rapporté que CCL23 et CCR1 sont impliqués dans le trafic de leucocytes et le développement de l'inflammation, les rôles exacts de ces deux protéines dans la leucémogenèse sont inconnus.

Pour illustrer les effets de la signalisation CCL23/CCR1 dans la leucémie causée par la fusion KMT2A-MLLT3, nous avons utilisé la technique de transfert d'énergie de résonance de bioluminescence 2 améliorée (ebBRET2) avec des tests d'immuno-empreintes. Nos résultats ont révélé que la signalisation de l'axe CCL23/CCR1 active plusieurs effecteurs de signalisation intermoléculaire, y compris Gi2, G12/13 et β-arrestine 1/2, mais avec un biais vers le recrutement de la β-arrestine. Nous avons également montré que le récepteur CCR1 présente une activité constitutive qui peut se coupler à une voie médiée par la protéine G et activer la voie impliquant les MAP kinases. Enfin, nous avons montré que la signalisation de l'axe CCL23/CCR1 provoque une activation de ERK1/2 dans les lignées cellulaires LMA potentiellement par une voie médiée par la β-arrestine.

Ces résultats indiquent que la signalisation de l'axe CCL23/CCR1 active plusieurs voies biologiques pouvant fournir des avantages majeurs pour le développement et la progression de la LMA et présentent ainsi CCL23 et CCR1 comme deux candidats intéressants pour une thérapie ciblée contre la LMA de type KMT2A-MLLT3.

Mots-clés : KMT2A-MLLT3, LMA, signalisation d'axe CCL23/CCR1, eBRET2, activation de la MAPK cascade, agonisme biaisé, activité constitutive de CCR1, signalisation dépendante de la β-arrestine.

Abstract

Acute Myeloid Leukemia (AML) is caused by abnormal proliferation of immature blood stem cells. Our lab focuses on an AML subgroup accounting for almost 20% of pediatric AML and characterized by a chromosomal translocation that generates the gene fusion: *KMT2A-MLLT3* (KM3). Interestingly, RNA-seq analysis of our KM3 AML model and AML patient samples has revealed that the chemokine CCL23 and its corresponding receptor CCR1 are highly upregulated in this disease. Although it has been reported that CCL23 and CCR1 are implicated in leukocyte trafficking and development of inflammation, the exact roles of these two proteins in leukemia are unknown.

To illustrate the effects of CCL23/CCR1 signaling in the KMT2A-MLLT3 rearranged leukemia we employed the enhanced bystander bioluminescence resonance energy transfer 2 (ebBRET2) technique along with phospho-immunoblots assays. Our results revealed that CCL23/CCR1 axis signaling activates multiple intermolecular signaling effectors, including Gi2, G12/13, and β-arrestin1/2 albeit with a bias towards β-arrestin recruitment. We also showed that the CCR1 receptor exhibits a constitutive activity which can couple to a G-protein mediated pathway to activate the MAPK cascade. Finally, we showed that CCL23/CCR1 axis signaling causes an activation of ERK1/2 in AML cell lines potentially through a β-arrestin-mediated pathway.

These results indicate that the CCL23/CCR1 axis signaling activates several biological pathways than can provide major advantages for the AML disease development and progression thus presenting both CCL23 and CCR1 as interesting candidates for targeted therapy against KMT2A-MLLT3 AML.

Keywords: KMT2A-MLLT3, AML, CCL23/CCR1 axis signaling, eBRET2, MAPK cascade activation, biased agonism, CCR1 constitutive activity, β-arrestin-dependent signaling.

Table of Contents

List of Tables

List of Figures

List of Abbreviations

HSC: Hematopoietic Stem Cell

AML: Acute Myeloid Leukemia

MLL: Mixed Lineage Leukemia

KMT2A: Histone-lysine N-methyltransferase 2A

AF9: ALL1-Fused Gene from Chromosome 9 Protein

MLLT3: Mixed-Lineage Leukemia Translocated to 3

KM3: KMT2A-MLLT3 Fusion

LEDGF: Lens Epithelium-Derived Growth Factor

SNL: Signal of Nuclear Localization

BRD: Bromodomain

PHD: Plant Homology Domains

TAD: Transactivation Domain

SET: Su(Var)3-9, Enhancer-of-zeste, Trithorax

SEC: Super Elongation Complex

DOT1L: Disruptor of Telomeric Silencing 1-Like

HSPC: Hematopoietic Stem and Progenitor Cell

ES: Embryonic Stem Cells

CB: Cord Blood

NSG: NOD Scid Gamma

B-ALL: B-Acute Lymphoblastic Leukemia

CCL23: CC Chemokine Ligand 23

RPKM: Reads Per Kilobase of transcript, per Million mapped reads

Cys: Cysteine Residue

GPCR: G Protein-Coupled Receptor

CCR1: CC Chemokine Receptor 1

PM: Plasma Membrane

BRET: Bioluminescence Resonance Energy Transfer

FRET: Förster Resonance Energy Transfer

YFP: Yellow Fluorescent Protein

GFP: Green Fluorescent Protein

Rluc: Renilla Luciferase

eYFP: Enhanced Yellow Fluorescent Protein

RlucII: Mutant Renilla Luciferase

eBRET2: Enhanced Bioluminescence Resonance Energy Transfer 2

rGFP: Renilla Green Fluorescent Protein

rGFP-CAAX: Renilla Green Fluorescent Protein fused to the CAAX Motif

ebBRET2: Enhanced Bystander Bioluminescence Resonance Energy Transfer 2

EMTA: ebBRET2 Membrane Translocation Assay

GRK2: GPCR Kinase 2

MAPK: Mitogen-Activated Protein Kinase

DMEM: Dulbecco's Modified Eagle Medium

FBS: Fetal Bovine Serum

PS: Penicillin Streptomycin Mix

RPMI: Roswell Park Memorial Institute

HA- M3R: Muscarinic Acetylcholine Receptor 3 tagged with 3 HA epitopes

HA-TPαR: Thromboxane A2 Receptor tagged with HA epitope

D2R: Dopamine D2 Receptor

DOR: Delta Opioid Receptor

PEI: Polyethylenimine

HBSS: Hank's Balanced Salt Solution

CCL3: CC Chemokine Ligand 3

CCL5: CC Chemokine Ligand 5

EGF: Epidermal Growth Hormone

PBS: Phosphate Buffer Saline

ANOVA: Analysis of Variance

p-ERK1/2: phosphorylated Extracellular Signal-Regulated Kinase1 and 2

PTX: Pertussis Toxin

I dedicate this thesis to my two-year-old niece, Sybille.

Your (half-scientist) uncle loves you so much.

Acknowledgements

First and foremost, I would like to thank Dr. Brian Wilhelm for welcoming me in his lab. I could not have asked for a better supervisor. Thank you for always being available, for giving me the resources and the room to learn, and for pushing me to be a better researcher.

Then, I would like to thank all the members of team Wilhelm. You guys gave me the motivation to come in to work every day. Thomas, thank you for being my friend and supporter. I had tons of fun sharing a desk with you for two years and without your amazing work I would not have had a project. Keep it up buddy! Elodie and Valerie thank you for your endless mentoring. I appreciated spending time with you in the lab and I am grateful for all the skills you taught me. Safia, thank you for being my savior when it came to bioinformatics. I hope I did not bother you too much with my jokes and singing in the office! Jessica, Blandine, and Benjamin, you guys are great colleagues and even greater researchers. I wish you all the best of luck in your future endeavors.

Also, I would like to thank Charlotte from the Bouvier Lab. God only knows how much I bothered you with my questions. Thank you for being so nice to me and taking the time to help whenever I needed. I am truly appreciative.

Likewise, I would like to thank the members of the Archambault lab, Myreille, Karine, Laia, and Damien. I enjoyed sharing the lab with you. Thank you for letting me borrow your kits and reagents.

I would like to thank Dr. Trang Hoang and Dr. Martin Sauvageau for accepting to evaluate my thesis.

Finally, I would like to express my profound gratitude for my family and friends. Anis, Rania, Line, Mays, and Besher, thank you for being the most loving and supporting family and for putting up with me all these years. Danielle, thank you for your infinite encouragement and love which gave the inspiration to finish writing my report. Finally, I would like to thank all my friends whose names were not mentioned. You know who you are. So much love and appreciation for you all.

Chapter 1. Introduction

1.1. Hemopoiesis and Leukemia

Hemopoiesis refers to the process by which blood cells are continually generated throughout the life of an individual. This process begins during embryonic development and continues throughout adulthood to produce and replenish the blood system[1]. During normal hemopoiesis, multipotent hematopoietic stem cells (HSC), located in the bone marrow, differentiate into more committed multipotent progenitor cells that eventually become restricted to either the myeloid or the lymphoid lineage[1]. The myeloid progenitors will normally further differentiate into fully committed red blood cells, platelets, macrophages, and granulocytes[1], whereas, lymphoid progenitors differentiate into natural killer cells and B type or T type lymphocytes (fig. 1).

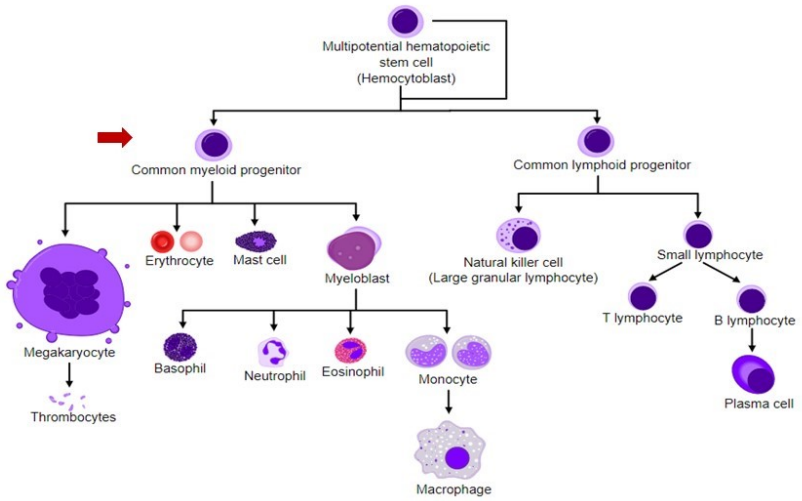

Figure 1. – Hemopoiesis Scheme.
During normal hemopoiesis in the bone marrow the hematopoietic stem cells (HSCs) divide and differentiate into either common myeloid or lymphoid progenitors. Ultimately, the myeloid progenitors further differentiate to give megakaryocytes, erythrocyte, mast cells, granulocytes, and macrophages. Whereas the lymphoid progenitors differentiate to give natural killer cells, B, and T lymphocytes. The red arrow points to the cell lineage affected by the acute myeloid leukemia (AML) disease. Adapted from Jagannathan-Bogdan *et al.*[2]

A leukemia develops when immature stem or progenitor blood cells lose their capacity to differentiate and continue to proliferate abnormally until they eventually outcompete normal stem cells in the bone marrow[3]. These malignant cells can then metastasize and invade the peripheral blood and other organs[3]. The different types of leukemia are classified according to the lineage/phenotype of the cells affected (e.g. lymphoid or myeloid) and depending on how quickly

the disease develops (acute or chronic). The acute leukemia starts abruptly, progresses very quickly (within a few days or a few weeks) and requires urgent treatment[3]. Chronic leukemia, on the other hand, develops rather slowly (in a few months) and may remain asymptomatic for a long time (latency period)[3].

1.2. Acute Myeloid Leukemia

Acute myeloid leukemia (AML) is a disease that disrupts the normal hemopoiesis resulting in poorly differentiated and rapidly dividing myeloid progenitor cells [4]. In patients, AML classically manifest as accumulations of myeloid blasts which expand in the bone marrow and the peripheral blood increasing the normal ratio of blasts by at least 20%[5]. Most AML patients present with a combination of leukocytosis and signs of bone marrow failure such as anemia and thrombocytopenia[5]. In addition, AML patients commonly exhibit fatigue, weight loss, and fever as symptoms[5]. Even though the majority of AML cases typically emerge in adult patients (average age ~68), this leukemia is considered the most prominent type of cancer threatening children under the age of 15 as it accounts for almost one third of the overall pediatric cancer cases[6-8].

One of the many challenges in understanding this sort of cancer is that AML is not a single disease but a highly genetically heterogenous one[5,9]. Elaborate cytogenetic analysis of AML patients revealed some to have normal karyotypes with recurring somatic mutations in genes, such as NPM1, RUNX1, FLT3, and DNMT3A[10], whereas, other patients showed complex karyotypes with frequent chromosomal translocations, such as t(8;21), inv(16)/t(16;16), and t(9;11)[11]. This genetic diversity accompanying AML gave rise to numerous clinical subgroups that are predictive of the disease prognosis and therapeutic outcomes (table I)[4]. Therefore, the classification of AML subgroups based on genetic lesions became a pivotal step to gain insight into leukemogenesis and disease progression.

Table 1. Genetic heterogeneity and disease prognosis of different AML subgroups.

Cytogenetic Abnormalities	Other Mutated Genes	Prognostic
AML with t(8:21) (q22;q22); RUNX1-RUNX1T1	N/A	Good
AML with inv (16) (p13;1q22); CBFB-MYH11	N/A	
AML with t(15;17)(q22; q12); PML-RARA	N/A	
CN-AML	NPM1	
CN-AML	CEBPA	
AML with t(9;11) (p21;q23); MLLT3-KMT2A	N/A	Intermediate
AML with t(8:21) (q22;q22); RUNX1-RUNX1T1	c-KIT	
AML with inv (3) (q21.3q26.2); GATA2, MECOM	N/A	Poor
AML with t(6;9) (p23;q34.1); DEK-NUP214	N/A	
CN-AML	KMT2A-PTD	
CN-AML	RUNX1	
CN-AML	TP53	
CN-AML	FLT3-ITD	
CN-AML	DNMT3A	

CN-AML: normal cytogenetics AML, N/A: not applicable. Adapted from De Kouchkovsky *et al.*[4]

1.3. KMT2A-MLLT3 Acute Myeloid Leukemia

Research in the Wilhelm lab is particularly focused on one AML subgroup, accounting for almost 20% of all pediatric AML cases[12]. This subgroup is characterized by a reciprocal translocation between chromosomes 9 and 11 (t(9;11)) which involves the rearrangement of a specific gene called *Histone-lysine N-methyltransferase 2A (KMT2A)*, also known as *Mixed-Lineage Leukemia (MLL)*[12,13]. Depending on the regions exchanged between the chromosomes 9 and 11, this translocation can result in the production of various chimeric proteins fusing the KMT2A protein to more than 120 different protein partners[14]. One of these partners, which is amongst the most prevalent, is encoded by the *Mixed-Lineage Leukemia Translocated to 3 (MLLT3)* gene, also known as *ALL1-Fused Gene from Chromosome 9 Protein (AF9)*. The *KMT2A-*

MLLT3 (KM3) gene fusion occurs following the precise rearrangement between the 21st band on the short arm of chromosome 9 and the 23rd band on the long arm of chromosome 11 (t(9;11)(p21;q23))[14]. The *KM3* gene fusion is itself sufficient to transform myeloid progenitor cells into leukemic blasts while other AML subtypes generally requires secondary mutations to drive the disease pathogenesis[15,16]. Furthermore, this fusion occurs in ~40% of KMT2A-rearranged pediatric AMLs and is generally correlated with an intermediate to poor prognosis by comparison to all KMT2A-rearranged leukemias[12,14].

1.3.1. KMT2A Protein

The human wild-type *KMT2A* gene encodes a multi-domain chromatin regulator that is ubiquitously expressed in HSCs[17]. This large protein is post-translationally cleaved by threonine aspartase-1 into two distinct modules[18]. The N-terminus (KMT2A-N) acts as a DNA binding module ushering the protein to attach at specific genes[17]. Whereas the C-terminus (KMT2A-C) acts as an epigenetic remodeler of the chromatin at the H3K4 and H3K27 sites controlling the transcription of target genes[19]. Together the N- and C-termini of the KMT2A protein typically regulate the expression of known master regulators of the HSC self-renewal and differentiation such as *HOXA* and *MEIS1* genes[17]. The KMT2A-N consists of a Menin-binding motif, a lens epithelium-derived growth factor (LEDGF)-binding domain, three AT-hooks, followed by two nuclear localization motifs (SNL1, SNL2) and a CXXC zinc-finger domain[20-22]. Additionally, KMT2A-N contains a bromodomain (BRD) and four plant homology domains (PHD fingers)[23,24]. The CXXC domain is crucial for binding to non-methylated CpG islands in the DNA allowing the KMT2A to be recruited to the loci of target genes[25]. Moreover, BRD and PHD fingers can recognize and bind to the chromatin to acetylate or methylate the lysine residues.[25]. The KMT2A-C module includes two chromatin modifying domains: a transactivation domain (TAD), followed by a SET [Su(Var)3-9, enhancer-of-zeste, trithorax] domain[26]. The former domain interacts with histone acetyltransferases that transfer acetyl groups to H3K27 site on the chromatin, while the latter domain catalyzes the transfer of a methyl group to the H3K4 site[26,27]. KMT2A-C is further assembled with other proteins such as WDR5, RBPB5 and ASH2L to form a larger KMT2A complex which enhances the KMT2A SET domain methyltransferase activity[26].

1.3.2 MLLT3 Protein

The human wild-type *MLLT3* gene encodes a relatively small protein expressed in a variety of tissues. The N-terminus (MLLT3-N) contains a YEATS domain which is a histone acetylation reader and part of the super elongation complex (SEC) targeting the complex to colocalize with RNA Pol II at a subset of actively transcribed genes[28]. In addition, independent from the elongation complex, the YEATS domain recognizes and binds the chromatin at the H3K9ac mark[28,29]. The C-terminus (MLLT3-C) comprises of three binding sites for the disruptor of telomeric silencing 1-like (DOT1L) methyltransferase[30]. DOT1L, when bound to MLLT3, is capable of mono-, di-, and tri-methylation of the chromatin at the H3K79 site regulating the transcription of target genes[30].

1.3.3. KMT2A-MLLT3 Fusion Protein

When the chromosomal rearrangement t(9;11) (p21;q23) takes place, it typically occurs with a break in the *KMT2A* gene at a breakpoint cluster region (BCR) between exon 8 and 12[31]. Consequently, the *KMT2A-C* terminus, coding for the TAD and SET domains, is excised, and replaced by the *MLLT3-C* terminus, coding for the three DOT1L binding sites. This results in the expression of the KMT2A-MLLT3 (KM3) fusion protein that has the gene-specific binding properties of the N-terminal portion of KMT2A, and the H3K79 methylation activity of C-terminal portion of MLLT3, via DOT1L (fig. 2)[32]. In turn, this leads to dysregulated constitutive transcription of KMT2A target genes, decreased differentiation of myeloid progenitors, and increased self-renewal of HSCs ultimately giving rise to AML[33].

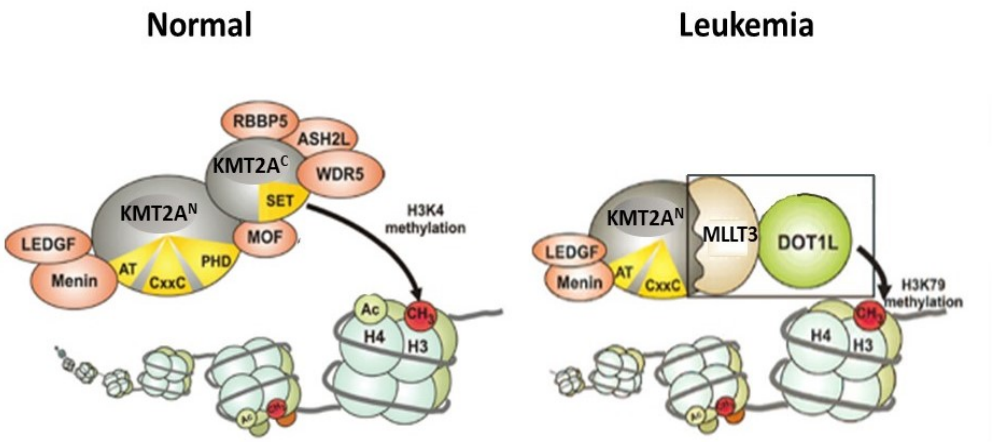

Figure 2. – KMT2A and KMT2A-MLLT3 Fusion Proteins.

In normal healthy individuals, the *KMT2A* gene encodes a large multi-domain protein divided into 2 distinct modules: N-terminal and C-terminal. The C-terminal has a SET domain which methylates the chromatin at the H3K4 active site. In leukemia patients with KMT2A-MLLT3 fusion, the entire KMT2A^{C} terminal is excised along with the PHD domain of the N-terminal. These are then replaced by the MLLT3 protein which recruits DOT1L to methylate the chromatin at the H3K79 active site instead. Adapted from Slany[34].

One would predict that the chromosomal rearrangement t(9;11) (p21;q23) would result in the expression of the reciprocal fusion protein joining the MLLT3-N terminus to the KMT2A-C terminus (MLLT3-KMT2A). A molecular characterization of 1590 KMT2A-rearranged biopsy samples obtained from acute leukemia patients revealed that an in-frame reciprocal fusion protein expression of MLLT3-KMT2A was only found in 25 of 295 biopsies of KM3 patients[35]. The fact that in most patients the reciprocal fusion MLLT3-KMT2A is likely not expressed strongly argues against any important role for this fusion in the acute myeloid leukemia transformation and progression[36]. Nevertheless, the N-terminal-truncated KMT2A-C protein resulting from t(9;11) was separately shown to exhibit oncogenic behaviors in *in vitro* culture systems[37]. Furthermore, several other reciprocal KMT2A fusions, such as the AF4(AFF1)–KMT2A fusion, have been shown to develop acute myeloid leukemia in transgenic mice[38]. Therefore, with the lack of clear experimental evidence, the functional role of the reciprocal fusion protein MLLT3-KMT2A in KM3 leukemogenesis remains an open question.

1.4. KMT2A-MLLT3 Acute Myeloid Leukemia Models

As stated previously, the vast heterogeneity of AML and the urge to identify key biological elements driving its leukemogenesis has motivated the development of model systems that can

recapitulate the human AML to allow for a better study of the disease. A wide range of such model systems have been developed over the last 3 decades and these are briefly reviewed here to provide context for the experimental work presented in this thesis.

1.4.1. Cell Lines

Amongst the first models to be tested were the *in vitro* cell lines, such as Molm-13 and Thp-1, derived from the extended *in vitro* culturing of KM3 AML patients leukemic cell samples[39,40]. Over the years such cell lines have provided a great deal of information about the disease drug sensitivity and are still utilized to this day in a variety of high-throughput assays[41]. One drawback of the cell lines as models for the AML disease is that the selection process used to derive these cell lines was based on their ability to grow in abnormal conditions outside their preferred microenvironments *(in vitro).* Therefore, these cells have acquired advantageous genetic mutations and biological profiles which do not mirror the disease seen in patients.

1.4.2. Murine Models

To overcome the limitation of cell line models and study the development of AML *in vivo,* murine models generated though the injection of oncogenic fusions into murine Hematopoietic Stem and Progenitor Cells (HSPCs) were developed. Due to the major advances in characterizing cell surfer markers of murine HSPCs in the late 90s, the identification of suitable HPSC cell populations required for such models made such efforts more feasible. Corral *et al.,* using the Cre-loxP mediated homologous recombination, were able to introduce the mouse *Kmt2a-Mllt3* gene fusion in murine embryonic stem (ES) cells[42]. They showed that these ES cells were able to transform and grow to develop a form of murine AML that can phenotypically mimic the human disease[42]. The creation of this murine model has provided a suitable setting upon which several key functional experiments were performed to define the genetic requirements of the KM3 leukemogenesis from normal progenitor cells. Despite murine models offering a powerful resource to study the KM3 AML, the problem remained with the leukemia origin being derived from murine cells which could present a selective condition altering the phenotype and/or the genotype of the disease from its human counterpart.

1.4.3. Human Models

Given the species differences between murine and human cells, the ability to generate *in vivo* models of KM3 leukemia starting from normal human HSCs, instead of murine HSCs, represented an interesting solution. In 2007, Barabé *et al.* achieved that by expressing the human *KM3* gene fusion via retroviral transduction in cord blood (CB) cells isolated from multiple infant donors. They then cultured the infected cells for an extended period and transplanted them into NOD Scid Gamma (NSG) immunodeficient mice[43]. After 3-4 months, the human cells in mice eventually developed either into AML or B-Acute Lymphoblastic Leukemia (B-ALL) blasts (fig. 3). The AML blasts isolated from these mice were phenotypically similar to human KM3 AML patient samples and were able to induce secondary myeloid leukemias when transplanted into healthy NSG mice, which is well-known trait of the KM3 AML patient samples[43].

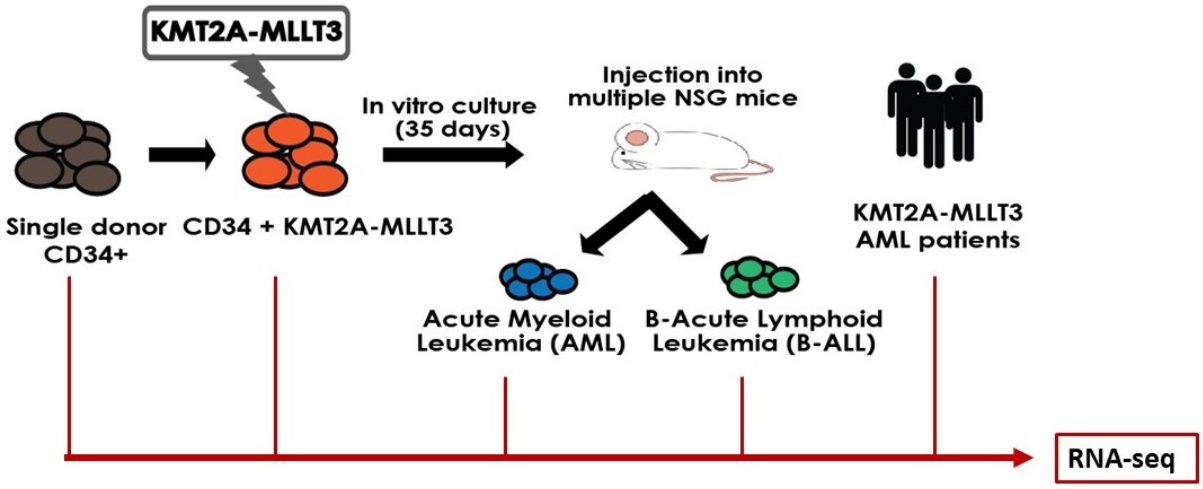

Figure 3. – KMT2A-MLLT3 AML Human Model.

CD34+ cells are isolated from the cord blood of a single infant donor. These cells are the transduced with the KMT2A-MLLT3 vector through retroviral transduction. After 35 days in culture, KMT2A-MLLT3 transduced CD34+ cells are injected into immunodeficient NSG mice. Within 2-3 months, these mice develop either B-acute lymphoid leukemia (B-ALL) or acute myeloid leukemia (AML). RNA-seq analysis was done at each step through the progression of the model. In parallel, RNA-seq was also done on KMT2A-MLLT3 pediatric AML patients. Adapted from Barabe *et al.*[16]

1.4.4. KMT2A-MLLT3 AML Biomarkers from the Human Model

In the Wilhelm lab, this previously mentioned KM3 AML human model has been studied extensively over the past decade. Through stepwise RNA-sequencing data generated using this

model, in parallel with samples obtained from KM3 AML patients (fig. 3), we have identified 39 biomarkers whose high expression level is specific to KM3 AML[16]. One of these biomarkers was the *CC Chemokine Ligand 23 (CCL23)* gene. The RNA-seq data analysis showed that *CCL23* was highly expressed in the KM3 transduced CB (CD34+KM3) cells *in vitro*, in the model AML (mAML) cells *in vivo*, and in the KM3 AML patient (pAML) samples. Interestingly, *CCL23* expression was absent in the initial CB ($CD34^+$) cells, in the model ALL (mALL) cells, and in the fully differentiated HSC (Leukocytes), implying that *CCL23* plays a crucial role in the KM3 AML progression (fig. 4)[16].

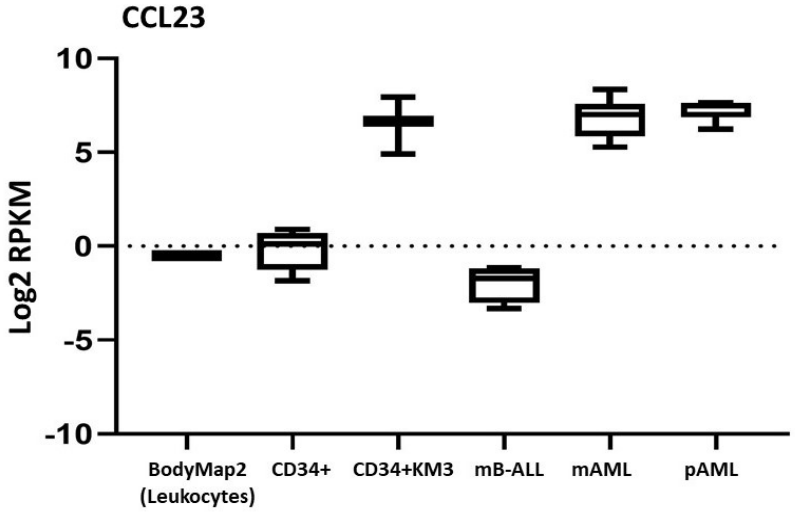

Figure 4. – CCL23 Differential Expression in KM3 AML Model and Patients.

Gene expression (log2 Reads Per Kilobase of transcript, per Million mapped reads (RPKM)) of *CCL23* in normal leukocytes (BodyMap2), normal HSC (CD34+) (n=5), HSCs infected with the KM3 fusion (CD34+KM3) (n=4), model B-ALL (mB-ALL) (n=5), model AML (mAML) (n=5) and patient samples (pAML) (n=40). Dashed horizontal line represents the threshold for a gene to be considered expressed. Adapted from Barabe *et al.*[16]

1.5. Chemokines and Their Receptors

1.5.1. Chemokines

The highly expressed *CCL23* gene encodes for a relatively small protein belonging to a large superfamily known as chemokines. Chemokines are secreted cytokines with selective chemoattractant properties which can bind and activate numerous receptors[44]. These small ligands have been implicated in various biological processes including the regulation of leukocyte trafficking, immunity, and hematopoiesis[45,46]. All 50 chemokines identified to date have an 7–12-kD molecular mass and exhibit 20–75% homology at the amino acid level[44]. Depending on the spacing of conserved cysteine residues present in the N-terminal, these ligands are subdivided into four distinct classes: (CXC), (CC), (XC), and (CX_3C) (fig. 5)[47]. In the CC, CXC, and CX3C subfamilies, the two Cysteine (Cys) residues are separated by 0, 1, and 3 residues, respectively, whereas in the XC subfamily the second Cys is absent from the sequence[47].

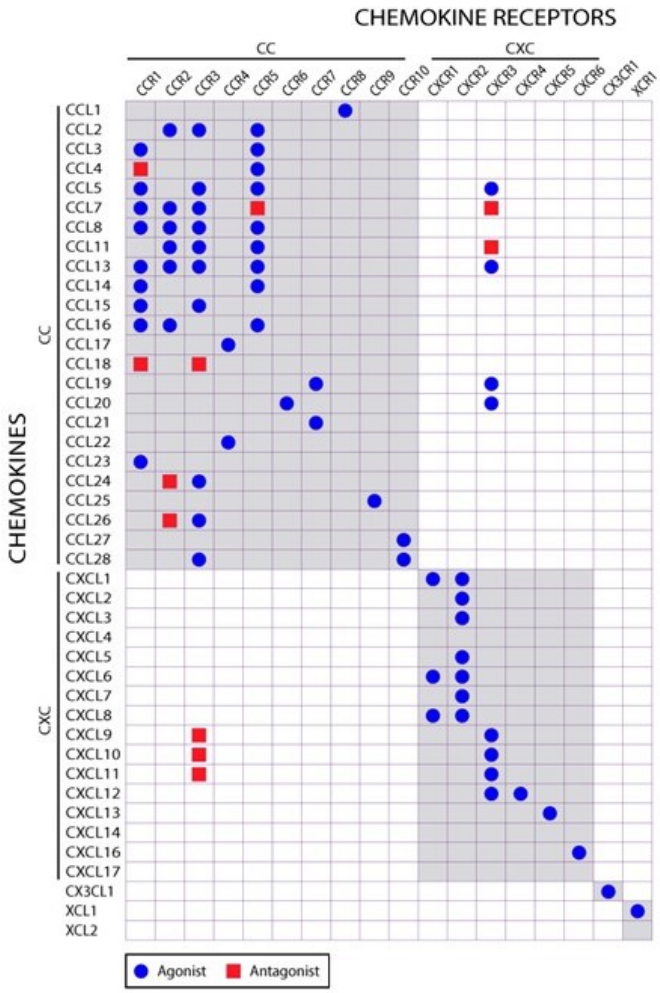

Figure 5. – The Human Chemokine-Receptor Network.

All identified chemokines and their respective receptors are listed under their specified class. The symbols signify whether the chemokines are considered as agonists (blue) or antagonist (red) of their respective receptors. Adapted from Stone *et al.*[48]

1.5.2. CC Chemokine Ligand 23 (CCL23)

CCL23 (also known as MPIF-1 and CKβ-8) is the most recent identified member of the large (CC) class of chemokines[49]. The human *CCL23* gene can give rise to distinct protein products due to alternative splicing and N-terminal processing[50]. CCL23 cDNA was initially isolated from a human aortic endothelial cell library and it encodes a 99 amino acids protein with a relatively long N-terminal sequence preceding the conserved cysteine pair when compared to other class CC chemokines[49]. This 99 amino acids CCL23 is studied in this project. In addition, an alternatively spliced form of CCL23 was discovered in the myeloid cell line Thp-1[51]. In this isoform, mRNA

uses a different splice acceptor resulting in the expression of a chemokine with an extra 18 amino acids[50]. CCL23 can also readily undergo post-translational proteolytic cleavage at its N-terminal which enhances its receptor binding capabilities[52].

A substantial number of *in vitro* studies demonstrate the functions of CCL23 to be highly dynamic depending on the cell and tissue type. CCL23 was originally characterized as a potent hematopoiesis suppressor inhibiting the colony formation ability of myeloid progenitors[49]. On a separate note, CCL23 secreted in the blood was discovered to employ pro-inflammatory responses by promoting leukocytes chemotaxis and directing the migration of monocytes, macrophages, and T-lymphocytes[49,51]. Similarly, this chemokine was able to enhance angiogenesis by boosting the migration capabilities of endothelial cells to ultimately induce tube formation[53]. Moreover, osteogenesis studies highlighted CCL23 as a potent chemoattractant for osteoclast precursors, but not for fully differentiated osteoclasts or osteoblasts[54]. Despite all this knowledge, further description of CCL23 functions, beyond *in vitro* assays, is halted because a *CCL23* gene homolog in mice has not yet been discovered, thus preventing the employment of loss-of-function tests in animal models[45].

In healthy individuals endogenous expression levels of CCL23 have been faintly detected in specific tissues such as the liver, the lung, and the appendix[51]. Nevertheless, transcripts of this chemokine become highly upregulated in several diseases and during inflammatory responses. It is now established that CCL23 is extremely produced in activated monocytes, eosinophils, and neutrophils upon treatments with specific inflammatory stimuli[55-57]. Additionally, CCL23 was detected in synovial fluids from rheumatoid arthritis patients, as well as in serum of systemic sclerosis patients[58,59]. Most recently, a study has shown that CCL23 is over-expressed and secreted in bone marrow and peripheral blood samples from patients with AML which coincides with our previous RNA-seq analysis[60].

1.5.3. Chemokines Receptors

To exert a signal through the cell, chemokines must bind and trigger suitable receptors. The human genome encodes about 20 different chemokine receptors (fig. 5). According to the class of chemokines for which they are selective, chemokine receptors are also subdivided into four distinct classes: (CCR, CXCR, XCR, and CX3CR; R indicates receptor)[61]. All chemokine receptors are transmembrane G protein-coupled receptors (GPCRs)[62]. These receptors belong to a large family

of signaling proteins that mediate cellular signaling in response to a great number of hormones, metabolites, cytokines, and neurotransmitters[48,63]. Upon binding of their associated ligands, GPCRs typically undergo conformational change which in turn induces a signalization cascade via different intracellular effectors, such as G proteins and β-arrestins[48]. G-proteins are heterotrimeric proteins composed by α, β and γ subunits, and are typically grouped depending on the similarity of their Gα subunit sequence[64]. 21 Gα subunits have been described in humans and they are divided into four main classes: Gαs, Gαi/o, Gαq/11 and Gα12/13 where each family can exert different responses in the cell[64,65]. β-arrestins effectors, on the other hand, belong to a superfamily of scaffolding proteins and are grouped into 2 distinct proteins, β-arrestins1 and β-arrestin2, and they mainly function to halt the activity of GPCRs[66].

1.5.4. CC Chemokine Receptor 1 (CCR1)

Most chemokines can bind and activate several chemokine receptors, however, the literature to date has shown that CCL23 is only capable of interacting with one receptor known as CC chemokine receptor 1 (CCR1)[48,67]. Remarkably, in our RNA-seq data analysis (fig. 3) we noticed that the *CCR1* gene expression was upregulated in the CD34+KM3, mAML, and pAML cells which was reminiscent of the *CCL23* gene expression profile (fig 4). However, *CCR1* was also highly expressed in normal leukocytes suggesting that this receptor could play an important role in the KM3 AML disease but cannot be viewed as one of its biomarkers (fig. 6).

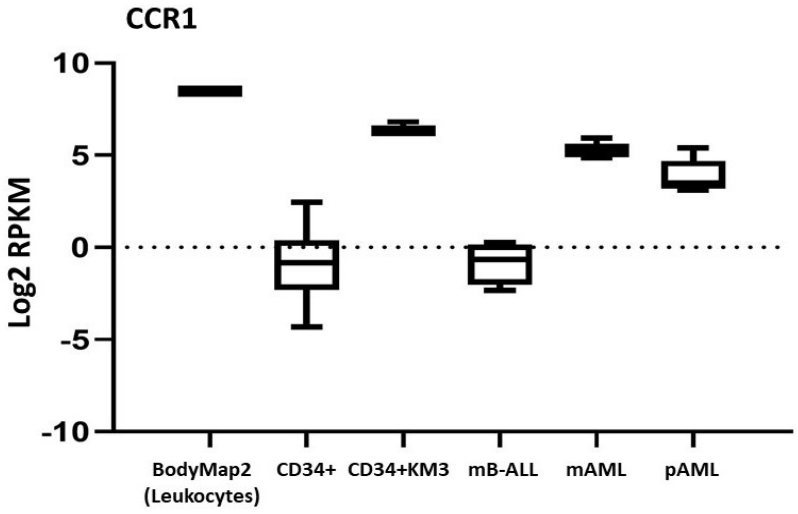

Figure 6. – CCR1 Differential Expression in KM3 AML Model and Patients.

Gene expression (log2 RPKM) of *CCR1* in normal leukocytes (BodyMap2), normal HSC (CD34+) (n=5), HSCs infected with the KM3 fusion (CD34+KM3) (n=4), model B-ALL (mB-ALL) (n=5), model AML (mAML) (n=5) and patient samples (pAML) (n=40). Dashed horizontal line represents the threshold for a gene to be considered expressed. Adapted from Barabe *et al.*[16]

CCR1 is the first human CC chemokine receptor to be identified at the cDNA level[68]. It is highly promiscuous with about 10 well-established ligands each with a different binding affinity[69]. Similar to other chemokines receptors, CCR1 can mainly activate the Gi class of G-proteins; i.e., they inhibit adenylate cyclase and limit the level of intracellular cAMP[70], however, it has been well documented that not all CCR1 ligands mediate the same signaling function. For instance, CCL3 and CCL5 appear to induce signal transductions through β-arrestins, whereas CCL14 and CCL15 activate the Gi pathways to inhibit adenylyl cyclase activity[67]. Thus, depending on the chemokine bound to its surface, CCR1 can elucidate distinct cellular responses, a phenomenon that has been dubbed as "biased agonism". Furthermore, CCR1 exhibits significant constitutive activity in its basal state (without ligand stimulation) which leads to its rapid internalization through the plasma membrane (PM), adding additional complexity to the CCR1 signaling potential[71].

In mice, gene deletions of CCR1 are not lethal but are able to elicit both beneficial and detrimental effects depending on the context of the tissue in question[72]. In humans, endogenous CCR1 is shown to be expressed on the surfaces of many inflammatory cells such as monocytes,

basophils, T cells, natural killer cells, and induced neutrophils[69,73]. Because the chemokine receptor is involved in regulating the chemotaxis of inflammatory cells, dysfunctional CCR1 has been implicated in many autoimmune diseases such as rheumatoid arthritis and multiple sclerosis[74,75]. Furthermore, the expression of this receptor has been observed in airway smooth muscle cells in the lung suggesting a possible role in asthma[76]. Also, it was found to be expressed in dystrophic neurons from patients with Alzheimer's dementia[77]. Finally, a new report investigating the upregulated GPCRs prevailing in AML patients reveals CCR1 to be amongst the most highly expressed, which is in agreement with our RNA-seq data[78].

1.6. Bioluminescence Resonance Energy Transfer (BRET)

The Bioluminescent Resonance Energy Transfer (BRET) technology is based on a resonance energy transfer between a light-emitting donor enzyme and a fluorescent acceptor protein. Since its characterization in 1999[79], this method became one of the most versatile techniques to examine protein-protein interactions in living cells and was quickly devoted to investigating the signaling of GPCRs and membrane receptors through drug screening assays. The BRET method is based on the Förster resonance energy transfer (FRET) occurring in some marine species, such as *Renilla reniformis*, which leads to a non-radiative energy transfer between an energy donor and an energy acceptor[80]. The energy donor is an enzyme called luciferase, which upon stimulation of its corresponding substrate, emits light at wavelengths typically corresponding to the blue light spectrum. On the other hand, the energy acceptor is a fluorophore which absorbs light at a given wavelength and reemits light at a longer wavelength that usually corresponds to either the yellow light spectrum, in case of the Yellow Fluorescent Protein (YFP), or to the green light spectrum, in the case of the Green Fluorescent Protein (GFP). The energy emitted by the acceptor relative to that emitted by the donor is termed as the BRET signal, or the BRET ratio.

To identify downstream effectors of membrane receptors such as GPCRs, the receptor of interest is generally fused to the energy acceptor, while the effector protein of interest is tagged to the energy donor. If the receptor and effector proteins do not interact, only light emitted from the substrate transformation by the energy donor can be monitored. But, if the two fusion proteins interact, they will come close together allowing for energy transfer between the donor and the acceptor resulting in an additional light emitted from the acceptor and an increase in the BRET signal.

1.6.1. Parameters for optimization of BRET

To satisfy the requirements for the BRET energy transfer, several parameters must be met (fig. 7). First, the emission spectrum of the donor must overlap with the excitation spectrum of the acceptor (fig. 7A)[81]. Second, the donor and acceptor should come in proximity of a minimum 10 nm which is the maximal distance for FRET (fig. 7B)[82]. At any distance longer than that, a BRET signal will not be observed. The third parameter has to do with the relative orientation of BRET partners. Due to the dipole-dipole nature of the resonance energy transfer mechanism, the donor and acceptor must be at an optimal orientation for the BRET to occur (fig. 7C)[83].

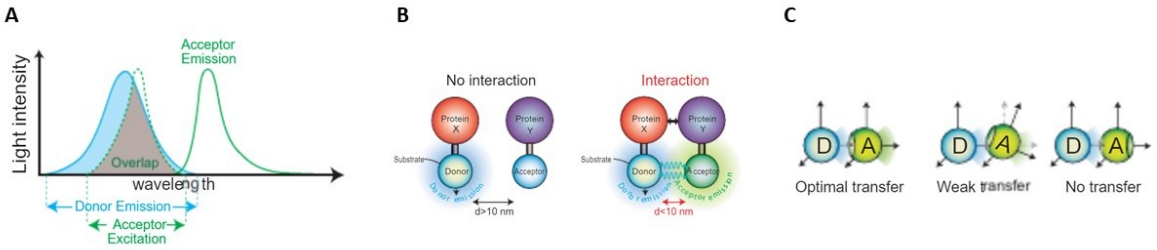

Figure 7. – Requirements of BRET Energy Transfer.

(A) To have energy transfer between the donor/acceptor couples, the donor emission spectrum must overlap with the excitation spectrum of the acceptor. **(B)** The energy transfer only occurs when the donor and acceptor come close at 10 nm or less. **(C)** The donor and acceptor must have optimal relative orientations for the energy to takes place. Adapted from Bacart *et al*[80].

1.6.2. Improved versions of BRET

Depending on the type of donor/acceptor couple and the substrate used to excite the donor, the BRET method can be divided into different versions (table II). The earliest described BRET version, now called BRET1, uses coelenterazine h as a substate for Renilla luciferase (Rluc) which in turn excites an enhanced YFP mutant (eYFP)[79]. The first variant of BRET1, is known as BRET2. In this version, DeepBlueC™ or coelenterazine 400a, a chemical derivative of coelenterazine h, is used to shift the maximal excitation wavelength of Rluc in order to stimulate GFP instead of EYFP[84]. BRET2 provides a better spectral separation between the donor and acceptor emission peaks which reduces the signal background noise observed in BRET1. Therefore, BRET2 is theoretically a better choice for screening assays. Additionally, an Rluc mutant (referred to in the results section as RlucII) has been recently described and obtained through consensus guided mutagenesis. This mutant contains 8 mutations from the original Rluc and they are A55T, C124A,

S130A, K136R, A143M, M185V, M253L, and S287L[85]. It was shown that this mutant increases the quantum yield when DeepBlueC™ is used as a substrate[86]. This mutant enzyme has since been implemented in the BRET2 version giving rise to the enhanced BRET2 (eBRET2)[86]. The last described BRET version, called BRET3, uses the Firefly luciferase enzyme from Photinus pyralis as a donor, DsRed fluorescent protein as an acceptor, and luciferin as a substrate[87,88]. However, current applications of the BRET3 assays are limited due to extremely weak signals and substantial overlap of donor and acceptor emission peaks.

Table 2. The versions of BRET

Version	Donor	Substrate	Donor Emission (nm)	Acceptor	Acceptor Emission (nm)
BRET1	Rluc	Coelenterazine	480	eYFP	530
BRET2	Rluc	Deep Blue C™	395	GFP	510
eBRET2	RlucII	Deep Blue C™	395	GFP	510
BRET3	Firefly	Luciferin	565	DsRed	583

1.6.3. eBRET2 Configurations Used in This Study

In this study we uniquely used the eBRET2 version albeit in two distinct configurations. In the first configuration, the GPCR of interest is expressed at the plasma membrane (PM) in its wild-type form. The energy donor, RlucII, is fused to the effector protein of interest while the energy acceptor Renilla Green Fluorescent Protein (rGFP) is anchored to the PM via a CAAX motif (rGFP-CAAX). If the GPCR activates the effector of interest upon ligand stimulation, this effector will be translocated to the membrane allowing RlucII to be in the proximity of rGFP leading to an energy transfer and an increase in the BRET signal. This configuration is called enhanced bystander BRET2 (ebBRET2) Membrane Translocation Assay (EMTA) (fig. 8)[89].

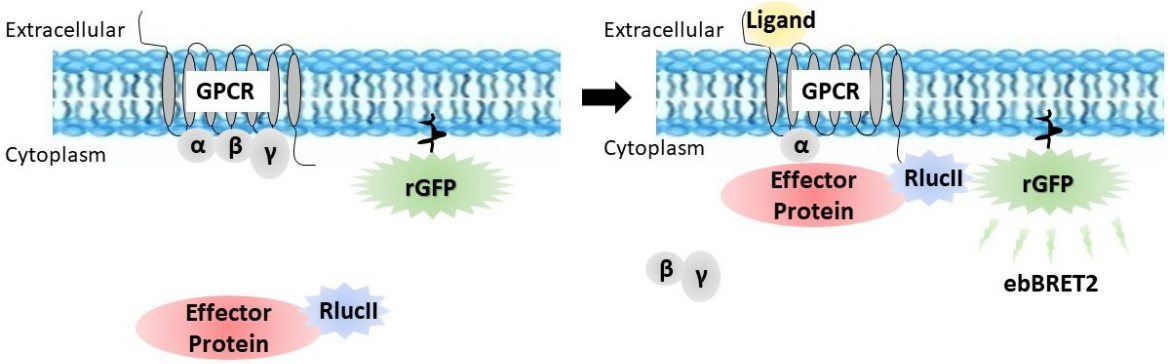

Figure 8. – ebBRET2 Membrane Translocated Assay (EMTA) biosensors.

The GPCR of interest is expressed at the plasma membrane in its wildtype form. The energy donor (RlucII) is fused to the effector protein of choice. The energy acceptor (rGFP) is anchored at the plasma membrane. Upon ligand stimulation, the GPCR elucidates a signal that activates the effector protein. The effector protein translocates to the plasma membrane allowing for an energy transfer and an increase in the (eBRET2) signal.

In the second configuration, the GPCR of interest is expressed at the PM in its wild-type form. The energy donor RlucII, is fused to the γ subunit of the G protein of interest while the energy acceptor, GFP10, is fused to GPCR Kinase 2 (GRK2) which is a known effector of Gβγ subunits[90]. After GPCR activation, the GRK2 forms a complex with the Gβγ subunits bringing RlucII near GFP10 which leads to an energy transfer and an increase in the BRET signal (fig. 9).

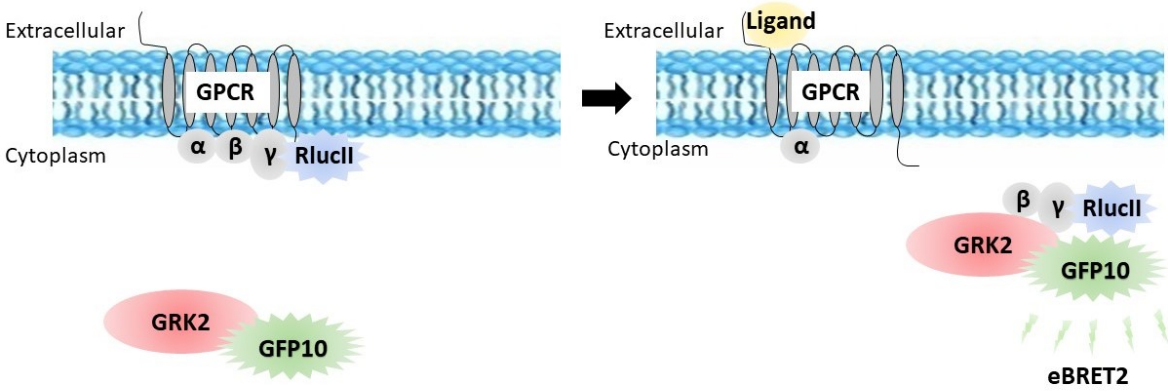

Figure 9. – The GRK2 biosensor.

The GPCR of interest is expressed at the plasma membrane in its wildtype form. The energy donor (RlucII) is fused to the Gγ subunit of the G protein of choice. The energy acceptor (GFP10) is fused to the GRK2 effector. After GPCR ligand activation, GRK2 forms a complex with Gβγ subunits allowing for an energy transfer and an increase in the (eBRET2) signal.

1.7. Research Hypothesis

Our RNA-seq data analysis revealed that the KMT2A-MLLT3 fusion prompts major expression changes in both human leukemia models and patients alike. We discovered that the gene encoding for the CCL23 chemokine becomes highly upregulated upon the introduction of KMT2A-MLLT3 to normal blood cells and continues to exhibit high expression levels at later stages of the disease, whereas in normal HSC and fully differentiated blood cells CCL23 is not expressed. Due to this differential expression, CCL23 was identified as a biomarker for KMT2A-MLLT3 AML disease (section 1.4.4). Interestingly, the gene encoding the chemokine receptor CCR1, which is a specific receptor of CCL23, displays similar expression profiles as it is also upregulated in the early and late stages of the human KMT2A-MLLT3 AML (section 1.5.4) although its expression is also upregulated in normal myeloid differentiation. This suggests that the expression of CCL23, which is directly or indirectly driven by the KMT2A-MLLT3 fusion, may allow the leukemia to co-opt the normal cellular machinery for differentiation (e.g. CCR1) to promote leukemic growth.

Together, these observations led us to hypothesize that CCL23 signaling through CCR1 may play a key role in the KM3 AML early transformation and may be essential for maintaining the disease progression at later stages.

1.8. The Main and Specific Research Objectives

In order to confirm the hypothesis, we set out to understand the different signaling pathways that the CCL23/CCR1 axis can activate.

To accomplish this objective, we devised it into two specific goals:

1) Identifying the early downstream effectors of CCR1 upon CCL23 stimulation.
2) Investigating the effects of CCL23/CCR1 axis signaling on the Mitogen-Activated Protein Kinase (MAPK) pathway.

Chapter 2. Materials and Methods

2.1. Cells

HEK293 clonal cell line (HEK293SL), hereafter referred to as (HEK293), and HEK293SL cells knock-out for β-arrestin1 and 2, hereafter referred to as (HEK293-ArrKO), were a generous gift from M. Bouvier (Université de Montréal, Montreal, Quebec, Canada) and are previously described[91,92]. Cells were cultured in Dulbecco's Modified Eagle Medium (DMEM, Gibco) supplemented with 10% fetal bovine serum (FBS, Wisent) and 1% penicillin-streptomycin mixture (100 U/mL penicillin and 100 µg/mL streptomycin (PS, Wisent). Cells were grown at 37ºC in 5% CO2 and 90% humidity.

Nomo-1, Thp-1, MonoMac-1, and Kg-1a cells (ATCC) were cultured in Roswell Park Memorial Institute (RPMI, Gibco) medium supplemented with 10% FBS (Wisent) and 1% of PS (Wisent). Cells were grown at 37ºC in 5% CO2 and 90% humidity.

All experiments were done using cells up to a maximal passage number of 40 times and discarded afterwards.

2.2. Plasmids and BRET constructs

The cDNA of human CCR1 (R&D Systems), human Muscarinic Acetylcholine Receptor 3 tagged with 3 HA epitopes (HA-M3R, cDNA resource center), human β-arrestin1 (cDNA Resource Center), human β-arrestin2 (cDNA Resource Center) and human Gα subunits of the different G proteins (cDNA resource center) were subcloned into pcDNA3.1(+) mammalian expression vector (Invitrogen) using restriction enzyme cloning method. Plasmids encoding βarrestin1-RlucII[93], βarrestin2-RlucII[94], rGFP-CAAX[89], GRK2-GFP10[95], Gγ5-RlucII[95], Gβ1[95], human Thromboxane A2 Receptor tagged with HA epitope (HA-TPαR)[96], human Dopamine D2 Receptor (D2R)[97], and human Delta Opioid Receptor (DOR)[98] are previously described and were a generous gift from M. Bouvier (Université de Montréal, Montreal, Quebec, Canada).

To selectively detect Gi activation, the plasmid encoding for the Rap1GAP-RlucII biosensor was a generous gift from M. Bouvier. In short, the construct coding for aa 1-142 of the effector Rap1 GTPase-activating protein (comprising a Gi/o binding domain) fused to Rluc8, was sequence-optimized, synthetized and subcloned at TopGenetech. From this construct, a RlucII tagged version of Rap1GAP (1-442) with a linker sequence (GSAGTGGRAIDIKLPAT) between

Rap1GAP and RlucII was created by Gibson assembly in pcDNA3.1(+) GFP10-RlucII, replacing GFP10. Three substitutions (i.e., S437A/S439A/S441A) at the protein kinase A of the Rap1GAP protein were introduced by PCR-mediated mutagenesis.[99] These mutations were introduced to eliminate any Gs-mediated Rap1GAP recruitment to the plasma-membrane.[100]

To selectively detect G12/13 activation, the plasmid encoding for PDZ-RhoGEF-RlucII was a generous gift from M. Bouvier. In short, a construct encoding the G12/13 binding domain of the human PDZ-RhoGEF (residues: 281-483) tagged with RlucII was done by PCR amplification from IMAGE clones (OpenBiosystems) and subcloned by Gibson assembly in pcDNA3.1(+) GFP10-RlucII, replacing GFP10. The peptidic linker GILREALKLPAT is introduced between RlucII and the G12/13 binding domain of PDZ-RhoGEF.[99]

2.3. Transfection

For BRET experiments, HEK293 cells (1.2 mL at 3.5×10^5 cells per mL) were transfected with a fixed final amount of pre-mixed biosensor-encoding DNA (1.2ug adjusted with an empty pcDNA3.1(+) plasmid). Cells were transfected using 1 mg/ml polyethylenimine 25kD linear (PEI, Polysciences) diluted in NaCl (150 mM, pH: 7.0) (3:1 PEI/DNA ratio). Cells were immediately seeded onto white, 96-well plates (Greiner Bio-one) at concentration of $3x10^5$ cells/well and maintained in DMEM containing 10% FBS and 1% PS.

For western blots experiments, HEK293 or HEK293-ArrKO were seeded in 6-well plates (Sarstedt) at a concentration of 100,000 cells/well. After 24hrs, cells are transfected with a pre-mixed DNA encoding for CCR1 and/or β-arrestin1 and/or β-arrestin2 (3ug adjusted with an empty pcDNA3.1(+) plasmid). Cells were transfected using 1 mg/ml polyethylenimine 25kD linear (PEI, Polysciences) diluted in Opti-MEM media (Gibco) (3:1 PEI/DNA ratio). 24hrs post transfection cells were serum deprived for 16hrs in 0% FBS DMEM.

2.4. Bioluminescence Resonance Energy Transfer Measurement

Enhanced BRET2 (eBRET2) was used to monitor the activation of each Gα protein, as well as βarrestin 1 and 2 recruitment to the plasma membrane. To scan for the G-proteins activation using the GRK2 biosensor, HEK293 cells were transfected with a mix of DNA expressing GRK2-GFP10, Gγ5-RlucII and Gβ1 along with the human, Gα12, Gα13, Gαi2, Gαq, Gαs, or Gα15 subunits and the tested receptor.

For βarrestin 1 and 2 recruitment testing using the EMTA biosensor, HEK293 cells were transfected with a mix of DNA expressing rGFP-CAAX and βarrestin1-RlucII or βarrestin2-RlucII along with the tested receptor. To investigate Gi activation using the EMTA biosensor, HEK293 cells were transfected with a mix of DNA expressing rGFP-CAAX and the Gi selective effector Rap1GAP-RlucII along with the human Gαi2 or Gαi3 subunits and the tested receptor. In the case of G12/13 activation using the EMTA biosensor, HEK293 cells were transfected with a mix of DNA expressing rGFP-CAAX and the G12/13 selective effector PDZ-RhoGEF-RlucII along with the human Gα12 or Gα13 subunits and the tested receptor.

On the day of experiment, 48hrs post transfection, cells were washed with pre-warmed PBS and then incubated at 37°c in Hank's Balanced Salt Solution (HBSS, Wisent; pH:7.4-7.6) for 1hr or otherwise specified. Cells were then stimulated with different concentrations of the tested ligands for 10mins. At the 5 minutes mark, cells were treated with the luciferase substrate, Deep Blue C™ (NanoLight Technologies) at a final concentration of 1uM. $BRET^2$ measurements were obtained using Trista^2 LB 942 (Berthold Technologies) microplate reader with a filter set (centre wavelength/band width) at 400 ± 70 nm and 515 ± 30 nm for detecting light emitted from RlucII (donor) and rGFP/GFP10 (acceptor) respectively. $BRET^2$ signal was calculated as the ratio of light intensity emitted by rGFP/GFP10 over the light intensity emitted by RlucII. For the GRK2 biosensor, $BRET^2$ measurements were further normalized by subtracting the ratio of basal conditions (without stimulation) from the ratio of stimulated conditions (after ligand binding) ($\Delta BRET^2 = BRET^2_{(stimulated)} - BRET^2_{(basal)}$).

Sources of the ligands and the concentrations used were as follows: CCL23 (GeneScript, 0.1μM or otherwise specified), CC Chemokine Ligand 3 (CCL3; GeneScript, 0.1μM or otherwise specified), CC Chemokine Ligand 5 (CCL5; GeneScript, 0.1μM or otherwise specified), U46619 (MilliporeSigma, 0.1μM), Dopamine (MilliporeSigma, 1μM), Carbachol (MilliporeSigma, 100μM), Met5-Enkephalin (MilliporeSigma, 100μM)

2.5. Protein Extraction and Immunoblotting

For HEK293 and HEK293-ArrKO, 48hrs post transfection cells were washed twice with PBS and serum starved in 0% FBS DMEM media overnight. Cells were then treated with either 0.1uM CCL23 or 100ng/uL human Epidermal Growth Hormone (EGF, R&D Systems) and

incubated at 37ºC for different time points (0-20mins). Cells were immediately washed with ice cold Phosphate Buffer Saline (PBS; pH:7.4).

For Nomo-1, Molm-13, Thp-1, MonoMac-1 and Kg-1a, cells were seeded at a density of $1x10^6$ cells/mL in T-25 flasks (Sarstedt) and serum starved in 0%FBS RPMI overnight. Cells were treated with 0.1uM CCL23 or 100ng/uL EGF and incubated at 37ºC for different time points (0-20mins). Following stimulation, $1x10^6$ cells were transferred into microcentrifuge tubes and immediately centrifuged in 4ºC for 3mins at 13,000rpm, washed with ice cold PBS, and centrifuged again.

To perform western blotting, cells were lysed using ice cold RIPA buffer (15mM Tris pH:7.5, 1mM EDTA, 1% NP-40 (ThermoFisher Scientific), 0.5% Sodium Deoxycholate, 0.1% SDS, 140mM NaCl, 1mM Na3VO4, 1% phosphatase inhibitor cocktail 2/3 (Sigma), 1X protease inhibitor Complete Mini EDTA-free (Roche)). Protein concentration was quantified using BCA protein assay (ThermoFisher Scientific). For western blotting, 20µg of proteins were separated on a 12% SDS-PAGE gel and transferred to nitrocellulose membranes (BioRad). The membranes were then blocked in 5% nonfat milk at room temperature for 1 h and incubated with the primary antibodies at room temperature for 1hr. Next, the horseradish peroxidase-conjugated secondary antibodies were used to incubate the membranes for 1hr. Finally, the membranes were visualized using Western ECL Chemiluminescence substrate (BioRad) and ChemiDoc XRS+ (BioRad). Gels were stripped for reprobing up to 2 times using a mild stripping buffer (1.5% Glycine, 0.1% SDS, 1% Tween 20, pH:2.2).

Sources of antibodies and the concentration used were as follows: goat anti-CCR1 (1:1000, Abcam, ab139399), rabbit anti-pERK1/2 (1:1000, New England Biolabs, 4370S), rabbit anti-ERK1/2 (1:2000, New England Biolabs, 4695S), rabbit anti-β-arrestin1/2 (1:1000, ThermoFisher Scientific, UA281915), mouse anti-GAPDH (1:5000, MilliporeSigma, 2742734), goat anti-mouse-HRP (1:20000, Jackson, 96596), goat anti-rabbit-HRP (1:10000, Jackson, 119181), rabbit anti-goat-HRP (1:5000, SantaCruz, sc-2768).

2.6. Statistical Analysis

All quantitative data were subjected to analysis of variance (ANOVA) or unpaired student t-test using the General Linear Model procedures of the Prism8 (GraphPad Software). Western blot

analyses of densitometry ratios were done using Image J (National Institutes of Health). All tests of significance were performed using the appropriate error terms according to the expectation of the mean squares for error. A p-value less than or equal to 0.05 was considered significant. Data are presented as means with the errors represented as standard error of the mean (SEM).

Chapter 3. Results

3.1. Validating the EMTA and GRK2 biosensors

Before using the eBRET2 sensors to investigate the CCL23/CCR1 signaling we needed to first validate their ability to function using our parameters. To do so, we selected a subset of GPCRs known to activate specific Gα subunits or β-arrestin proteins upon stimulation with different pharmacological agonists. To test for Gαi activation, human dopamine receptor (D2R) was chosen due to its effective Gαi coupling ability[101]. HEK293 were transfected with D2R and the Rap1GAP-RlucII biosensor along with either Gαi2 or Gαi3 subunits. As expected, Dopamine stimulation resulted in significant activation of both subunits indicated by the increase in the BRET2 signal when compared to cells lacking the of Gα subunits overexpression (fig 10A). Human Thromboxane A2 Receptor (TPαR) was chosen to test for the Gα12/13 activation due to its strong Gα12/13 coupling ability[102]. HEK293 overexpressing TPαR, PDZ-RhoGEF-RlucII biosensor, and either the Gα12 or Gα13 subunit were stimulated with the thromboxane mimic, U46619. As expected, the stimulation resulted in substantial activation of both Gα12 and Gα13 revealed by the increase in BRET2 signal when compared to cells not expressing the Gα subunits (fig 10B). For β-arrestin1/2 recruitment, the human Delta Opioid Receptor (DOR) was used as it is shown to potently recruit β-arrestin proteins for subsequent cellular signaling[103]. HEK293 were transfected with DOR along with either β-arrestin1-RlucII or β-arrestin2-RlucII biosensors. As expected, stimulation with the opioid, Met5-Enkephalin, resulted in potent recruitment of β-arrestin1 and 2 observed through the increase of the BRET2 signal (fig 10C).

To test the proper functioning of the GRK2 biosensor, D2R receptor and human Muscarinic Acetylcholine Receptor 3 (M3R) were used to detect the Gαi and Gαq activation, respectively. M3R was chosen as it is shown to strongly activate Gαq proteins after ligand stimulation[104]. As expected, Carbachol stimulation in HEK293 cells overexpressing the biosensor, M3R, and the Gαq subunit, caused an activation of the Gαq protein evident by the increase in the ΔBRET2 signal (Basal vs Stimulated conditions; *see materials and methods section*) in comparison to cells not expressing the Gαq subunit (fig 10D). Similar results were obtained in HEK293 cells overexpressing D2R and Gαi2 subunits upon stimulation with Dopamine (fig 10E).

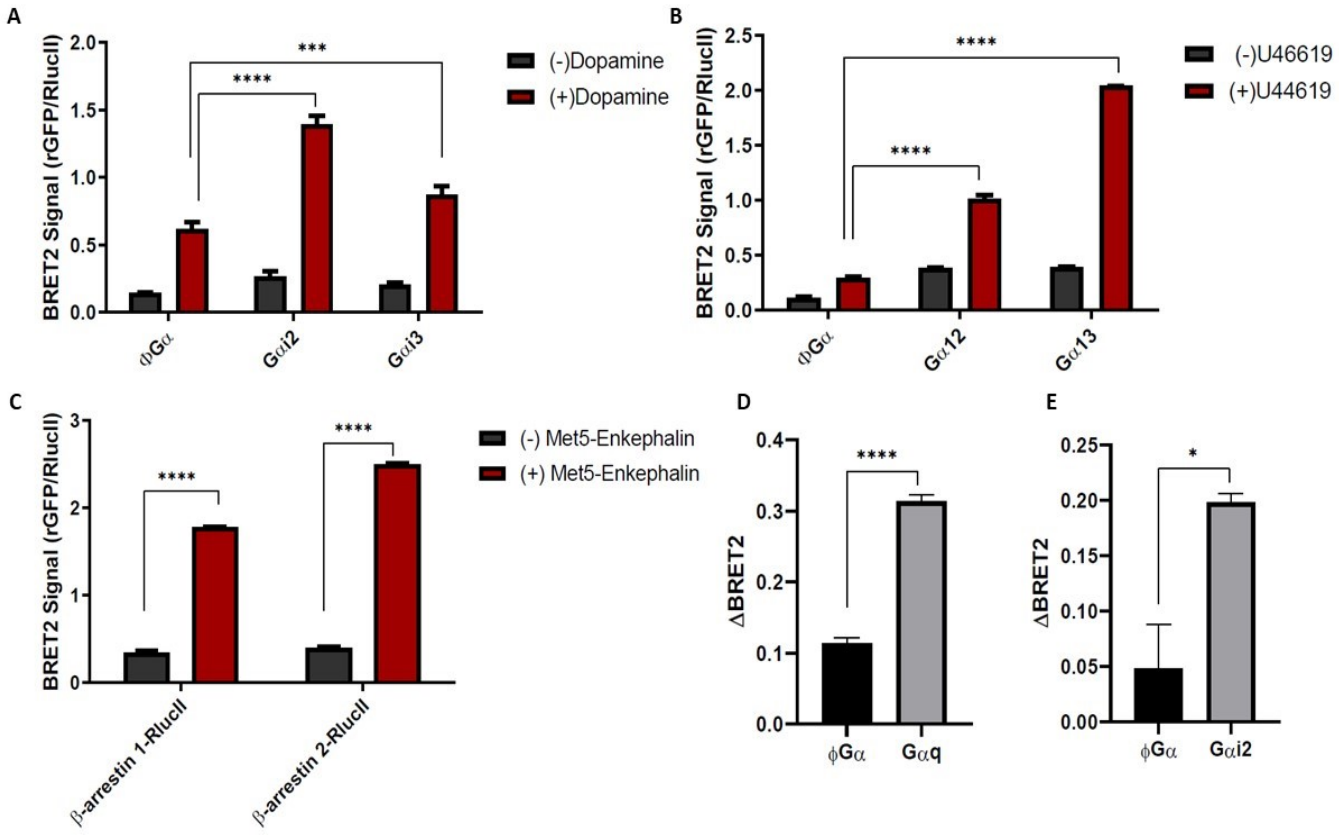

Figure 10. – Validation of the eBRET2 biosensors.

(A) HEK293 cells were transfected with RapGAP-RlucII, rGFP-CAAX and D2R along with or without Gαi2/i3. Cells were incubated at 37ºC for 10 minutes in the presence or absence of Dopamine (1μM). **(B)** HEK293 cells were transfected with PDZ-RhoGEF-RlucII, rGFP-CAAX and TPαR along with or without Gα12/13. Cells were incubated at 37ºC for 10 minutes in the presence or absence of U46619 (10nM). **(C)** HEK293 cells were transfected with β-arrestin1/2-RlucII, rGFP-CAAX and DOR. Cells were incubated at 37ºC for 10 minutes in the presence or absence of Met5-Enkephalin (100μM). **(D, E)** HEK293 cells were transfected with GRK2-GFP10, rGFP-CAAX, Gγ3-RlucII, Gβ1 and the α subunits of the indicated G proteins along with M3R **(D)** or D2R **(E)**. Cells were incubated at 37ºC for 10 minutes in the presence or absence of Carbachol (100uM) **(D)** or Dopamine (1uM) **(E)**. Raw $BRET^2$ ratios and $\Delta BRET^2$ = (BRETLigand – BRETBasal) measurements are means ± s.e.m of at least two independent experiments plotted using GraphPad Prism® (GraphPad Software). The statistical significance was calculated using an unpaired Student's t test for **(D, E)** or two-way analysis of variance (ANOVA) with Tuckey's post-test for **(A, B, C).** *, $p < 0.05$; ***, $p = 0.0002$; ****, $p < 0.0001$.

These results highlighted the ability of the EMTA and GRK2 biosensors to detect Gα and β-arrestin protein activation and confirmed that they could be utilized for subsequent characterization of the CCL23/CCR1 signaling network.

3.2. Examining the signalling effects of CCL23/CCR1, CCL3/CCR1, and CCL5/CCR1 axes by the ebBRET2 biosensors.

3.2.1. Detecting the CCL23/CCR1 axis effects by the GRK2 biosensor.

After testing the effectiveness of the biosensors, we next wanted to determine which G proteins are activated by CCR1 when stimulated with CCL23. We therefore decided to use the GRK2 biosensor as a rapid method to scan all the G protein families for potential coupling. We selected a subset of Gα subunits to represent each of the 5 families of G proteins as follows: Gαi2 (Gαi family), Gαq and Gα15 (Gαq family), Gαs (Gαs family) and Gα12 (Gα12/13 family). HEK293 cells were transfected with GRK2 biosensor and CCR1 along with (or without) the indicated Gα subunits and then treated with CCL23. These results revealed that, although not statistically significant, the CCL23/CCR1 axis has the tendency to increase the $\Delta BRET^2$ (Basal vs Stimulated conditions; *see materials and methods section*) signal for both the Gαi2 and Gα12 subunits when compared to cells not expressing the Gα subunits. Whereas no increase in $\Delta BRET^2$ was observed for any of the other Gα subunits (fig 11).

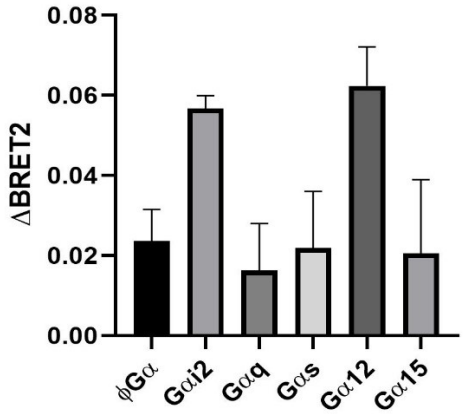

Figure 11. – Gα protein scanning using the GRK2 biosensor.

HEK293 cells were transfected with CCR1, Gγ3-RlucII, GRK2-GFP10 and Gβ1 along with the α subunits of the indicated G proteins. Cells were incubated at 37°C for 10 minutes in the presence or absence of CCL23 (100nM). $\Delta BRET^2$ measurements are means ± s.e.m of two independent experiments plotted using GraphPad Prism® (GraphPad Software).

3.2.2. Optimizing the EMTA biosensors for the study of CCL23/CCR1 signaling effects.

Because the G-protein scanning showed that CCL23/CCR1 axis can potentially activates the Gαi and Gα12/13 families of G proteins, we wanted to use the EMTA biosensors to further test the activation of different α subunits within the Gαi and Gα12/13 families in addition to the β-arrestin1/2 proteins. To obtain the best $BRET^2$ signal, the DNA quantities of transfection for each EMTA biosensor had to be optimized first. To achieve that, we transfected HEK293 cells were with fixed amounts of the plasmid expressing the effector protein of interest fused to the energy donor (RlucII) in addition to fixed amounts of the plasmid expressing the energy acceptor (rGFP-CAAX) along with increasing amounts of the plasmid expressing the receptor (CCR1). In another condition, we transfected HEK293 cells with fixed amounts of the effector protein of interest fused to the energy donor (RlucII) in addition to fixed amounts of the plasmid expressing the receptor (CCR1) along with increasing amounts of the plasmid expressing the energy acceptor (rGFP-CAAX). Cells were then stimulated with CCL23 and the BRET2 signal was detected (fig 12).

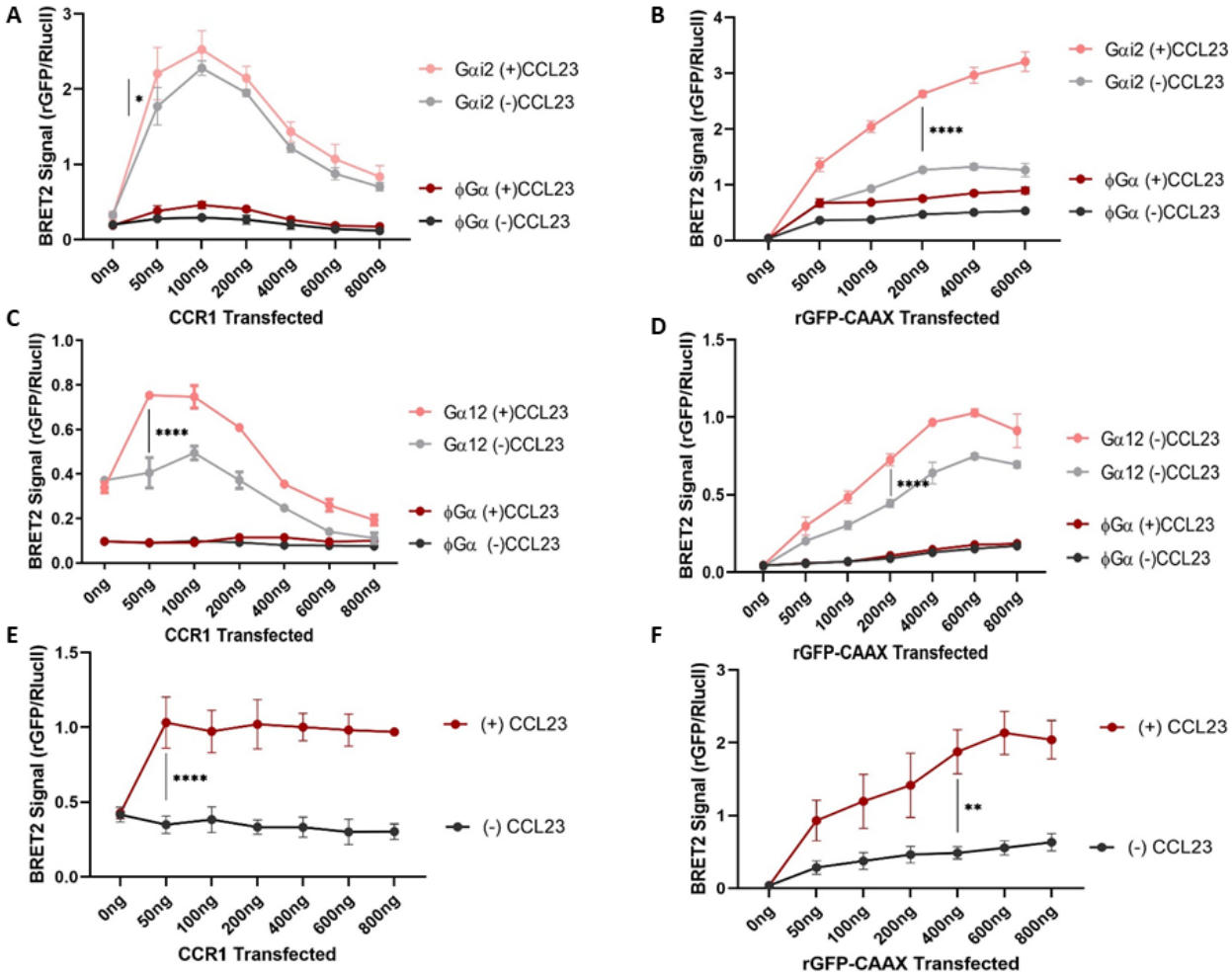

Figure 12. – EMTA biosensors optimization.

(A, B) HEK293 cells were transfected with Rap1GAP-RlucII and with or without Gαi2 along with **(A)** increasing amounts of CCR1 or **(B)** increasing amounts of rGFP-CAAX. **(C, D)** HEK293 cells were transfected with PDZ-RhoGEF-RucII and with or without Gα12 along with **(C)** increasing amounts of CCR1 or **(D)** increasing amounts of rGFP-CAAX. **(E, F)** HEK293 cells were transfected with the β-arrestin2-RlucII along with **(E)** increasing amounts of CCR1 or **(F)** increasing amounts of rGFP-CAAX. Cells were incubated at 37ºC for 10 minutes in the presence or absence of CCL23 (100nM). Raw BRET ratios are means ± s.e.m of two independent experiments plotted using GraphPad Prism® (GraphPad Software). The statistical significance was calculated using two-way ANOVA with Tuckey's post-test. *, $p < 0.05$; **, $p = 0.002$; ****, $p < 0.0001$.

These optimization experiments showed that the ideal amount of the CCR1 expressing plasmid to transfect the HEK293 cells was ~50ng. This amount resulted in the most significant increase in the BRET^2 signal after stimulation with CCL23 for all three biosensors: Rap1GAP-RlucII, PDZ-RhoGEF-RlucII, and β-arrestin2-RlucII (fig 12A, C, E). Regarding the amount of plasmid expressing the rGFP-CAAX, 200ng was selected as the optimal amount for both the PDZ-RhoGEF-RlucII and Rap1GAP-RlucII biosensors (fig 12B, D), whereas 400ng of the β-arrestin2-

RlucII biosensor plasmid was needed for an optimal increase in the BRET^2 signal upon CCL23 stimulation (fig 12F).

3.2.3. Detecting the CCL23/CCR1 signalling effects by the EMTA biosensors.

After choosing the DNA quantities that gave the best window of response (unstimulated vs stimulated signal), we carried out dose response experiments where we transfected HEK293 cells with the EMTA biosensors, CCR1, and the different Gα subunits and stimulated the cells with increasing concentrations of CCL23 (fig 13).

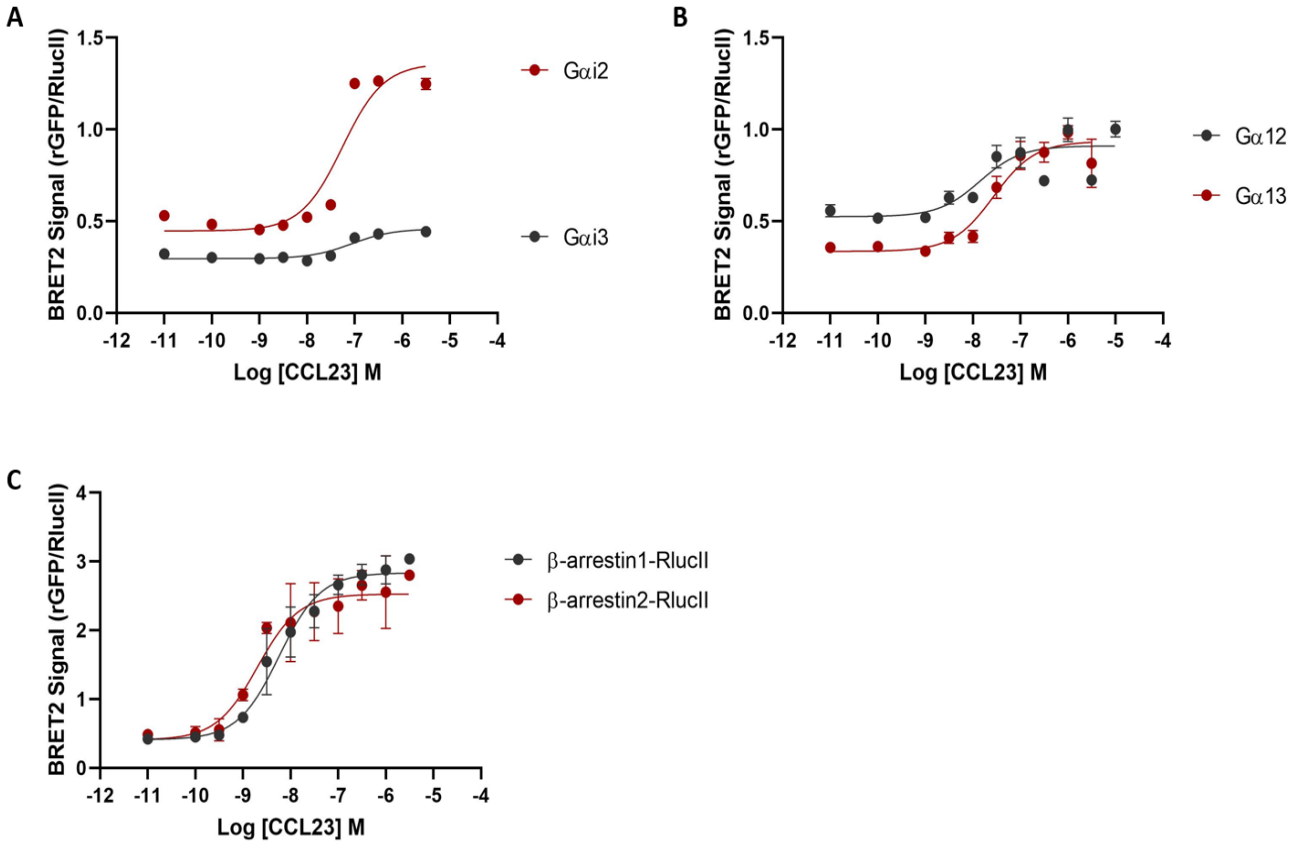

Figure 13. – CCR1 dose dependent activation of downstream effectors upon simulation with CCL23.

(A) HEK293 cells were transfected with CCR1, RapGAP-RlucII, and rGFP-CAAX along with Gαi2 or Gαi3. **(B)** HEK 293 cells were transfected with CCR1, PDZ-RhoGEF-RlucII, and rGFP-CAAX along with Gα12 or Gα13. **(C)** HEK293 cells were transfected with CCR1 and rGFP-CAAX along with β-arrestin1-RlucII or β-arrestin2-RlucII. Cells were incubated at 37°C for 10 minutes in the presence of indicated concentrations of CCL23. Raw BRET ratios are means ± s.e.m of three independent experiments plotted and analyzed using GraphPad Prism® (GraphPad Software).

These results demonstrated that the CCL23/CCR1 axis signaling caused a dose-dependent increase of the BRET2 signal when activating the Gαi2 (fig 13A), Gα12 and Gα13 (fig 13B), β-arrestin1 and β-arrestin2 (fig 13C) biosensors. By comparing the relative EC_{50} values of the BRET2 signal across each of these biosensors (table 3), we observed that the β-arrestin1/2 biosensors required lower concentrations of CCL23 to reach EC_{50} (2.75E-08, 2.02E-09 (M)) than the Gαi2/i3 (5.54E-08, 8.77E-08 (M)) and the Gα12/13 (2.25E-08, 2.75E-08 (M)) biosensors. Also, by comparing the relative E_{max} values obtained from the Gαi2/i3 biosensor we observe that CCL23/CCR1 signaling showed a higher span of the BRET2 signal when activating the Gαi2 biosensor (0.91) in comparison to activating the Gαi3 biosensor (0.16) (table 3, fig 13A). However, the E_{max} values were close between the Gα12/13 (0.46, 0.60) biosensors and the β-arrestin1/2 (2.43, 2.12) biosensors.

Table 3. EC50 and Emax values of CCL23/CCR1 signaling

Gαi2 Signaling		Gαi3 Signaling		Gα12 Signaling		Gα13 Signaling		β-arrestin1 Recruitment		β-arrestin2 Recruitment	
EC_{50}	**E_{max}**	**EC_{50}**	**E_{max}**	**EC_{50}**	**E_{max}**	**EC_{50}**	**E_{max}**	**EC_{50}**	**E_{max}**	**EC_{50}**	**E_{max}**
5.54E-08 M	0.91	8.77E-08 M	0.16	2.25E-08 M	0.46	2.75E-08 M	0.60	5.75E-09 M	2.43	2.02E-09 M	2.12

3.2.4. Comparing the signaling effects of CCL23/CCR1, CCL3/CCR1, and CCL5/CCR1 axes.

To fully characterize the signaling potential of CCL23 through CCR1, we decided to test whether CCL23 exhibits a signaling bias when compared to other CCR1 chemokines. Therefore, we repeated the dose-response experiments, using the same DNA quantities described earlier for transfection, but in this case, we simulated with increasing concentrations of two alternative chemokines, CCL3 and CCL5 (fig 14).

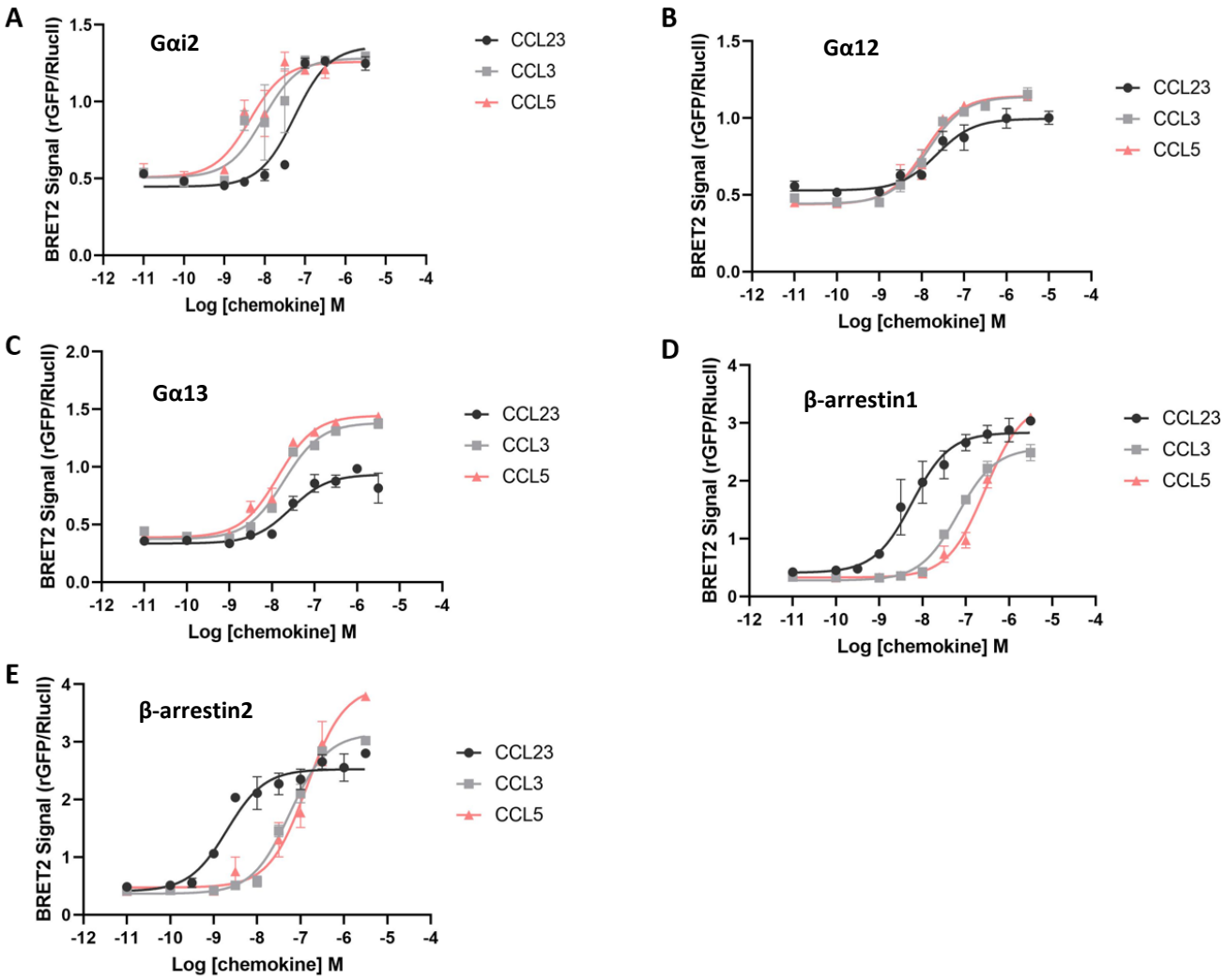

Figure 14. – CCR1 dose dependent activation of downstream effectors upon simulation with different chemokines.

(A) HEK293 cells were transfected with CCR1, RapGAP-RlucII and rGFP-CAAX along with Gαi2. **(B, C)** HEK293 cells were transfected with CCR1, PDZ-RhoGEF-RlucII and rGFP-CAAX along with **(B)** Gα12 or **(C)** Gα13. **(D, E)** HEK293 cells were transfected with CCR1 and rGFP-CAAX along with **(D)** β-arrestin1-RlucII or **(E)** β-arrestin2-RlucII (b). Cells were incubated at 37ºC for 10 minutes in the presence of indicated concentrations (log M) of the chemokines CCL23, CCL3, and CCL5. Raw BRET ratios are means ± s.e.m of at least three independent experiments plotted using GraphPad Prism® (GraphPad Software).

These assays showed that the signaling of the CCL3/CCR1 and CCL5/CCR1 axes, similar to CCL23/CCR1, caused a dose-dependent increase of the BRET2 signal when activating the Gαi2 (fig 14A), Gα12 (fig 14B), Gα13 (fig 14C), β-arrestin1 (fig 14D), and β-arrestin2 (fig 14E) biosensors. A comparison of the EC_{50} and E_{max} values of the BRET2 signal across the three

chemokines was done in table 4. For activating the Gαi2 biosensor, CCL23 had similar E_{max} values to CCL3 and CCL5 (0.91, 0.78, 0.75, respectively). However, CCL23 required higher concentrations to reach the EC_{50} value (5.54E-08 M) than CCL3 and CCL5 (9.34E-09, 4.36E-09 M) (table 4, fig 14A). In the case of the Gα12 biosensor activation, CCL23 exhibited similar EC_{50} values to CCL3 and CCL5 (2.25E-08, 1.40 E-08, 1.20 E-08 M, respectively), but decreased E_{max} values (0.46) relative to CCL3 and CCL5 (0.70, 0.70) (table 4, fig 14B). Parallel results were observed for the Gα13 biosensor activation as CCL23, CCL3 and CCL5 recorded EC_{50} values of (2.75E-08, 1.91E-08, 1.39E-08 M, respectively) and E_{max} values of (0.60, 1.00, 1.06, respectively) (table 4, fig 14C). When it came to the β-arrestin1 biosensor activation, we observed that the E_{max} values were similar between CCL23 (2.43), CCL3 (2.29), and CCL5 (3.04). Nonetheless, CCL23 required lower concentrations to reach the EC_{50} value (5.75E-09 M) than CCL3 and CCL5 (6.55E-08, 2.81E-07 M) (table 4, fig 14D). Lastly, the β-arrestin2 biosensor activation, similar to the β-arrestin1 biosensor activation, showed that CCL23 required lower concentrations to reach the EC_{50} value (2.02E-09 M) than CCL3 and CCL5 (5.65E-08, 1.39E-07 M). Finally, the E_{max} values assessment of the β-arrestin2 biosensor activation uncovered that CCL23 (2.12) recorded closer values to CCL3 (2.78) than CCL5 (3.49) (table4, fig 14E).

Table 4. EC50 and Emax values of chemokines signaling through CCR1

	Gαi2 Signaling		Gα12 Signaling		Gα13 Signaling		β-arrestin1 Recruitment		β-arrestin2 Recruitment	
Chemokine	**EC_{50}**	**E_{max}**	**EC_{50}**	**E_{max}**	**EC_{50}**	**E_{max}**	**EC_{50}**	**E_{max}**	**EC_{50}**	**E_{max}**
CCL23	5.54E-08 M	0.91	2.25E-08 M	0.46	2.75E-08 M	0.60	5.75E-09 M	2.43	2.02E-09 M	2.12
CCL3	9.34E-09 M	0.78	1.40 E-08 M	0.70	1.91E-08 M	1.00	6.55E-08 M	2.29	5.65E-08 M	2.78
CCL5	4.36E-09 M	0.75	1.20 E-08 M	0.70	1.39E-08 M	1.06	2.81E-07 M	3.04	1.39E-07 M	3.49

3.3. Uncovering CCR1 constitutive activity using the EMTA biosensors

CCR1 has been reported to exhibit basal activity (or "constitutive activity") where the receptor can initiate downstream signaling without the stimulation of any agonist[71]. To explore this notion with our EMTA biosensors, we transfected the HEK293 cells with the different biosensors either after the expression of CCR1 or without it. Then, we measured the BRET2 signal after incubating the cells for an extended period in serum-free HBSS medium to eliminate the existence of any nutrient that could theoretically stimulate the receptor. We observed that the expression of CCR1 in HEK293 cells, when compared to HEK293 cells not expressing the receptor, caused a significant increase in the BRET2 signal only in the presence of Gαi2 subunit biosensor. None of the other subunits or effectors showed a significant increase of the signal (fig 15A).

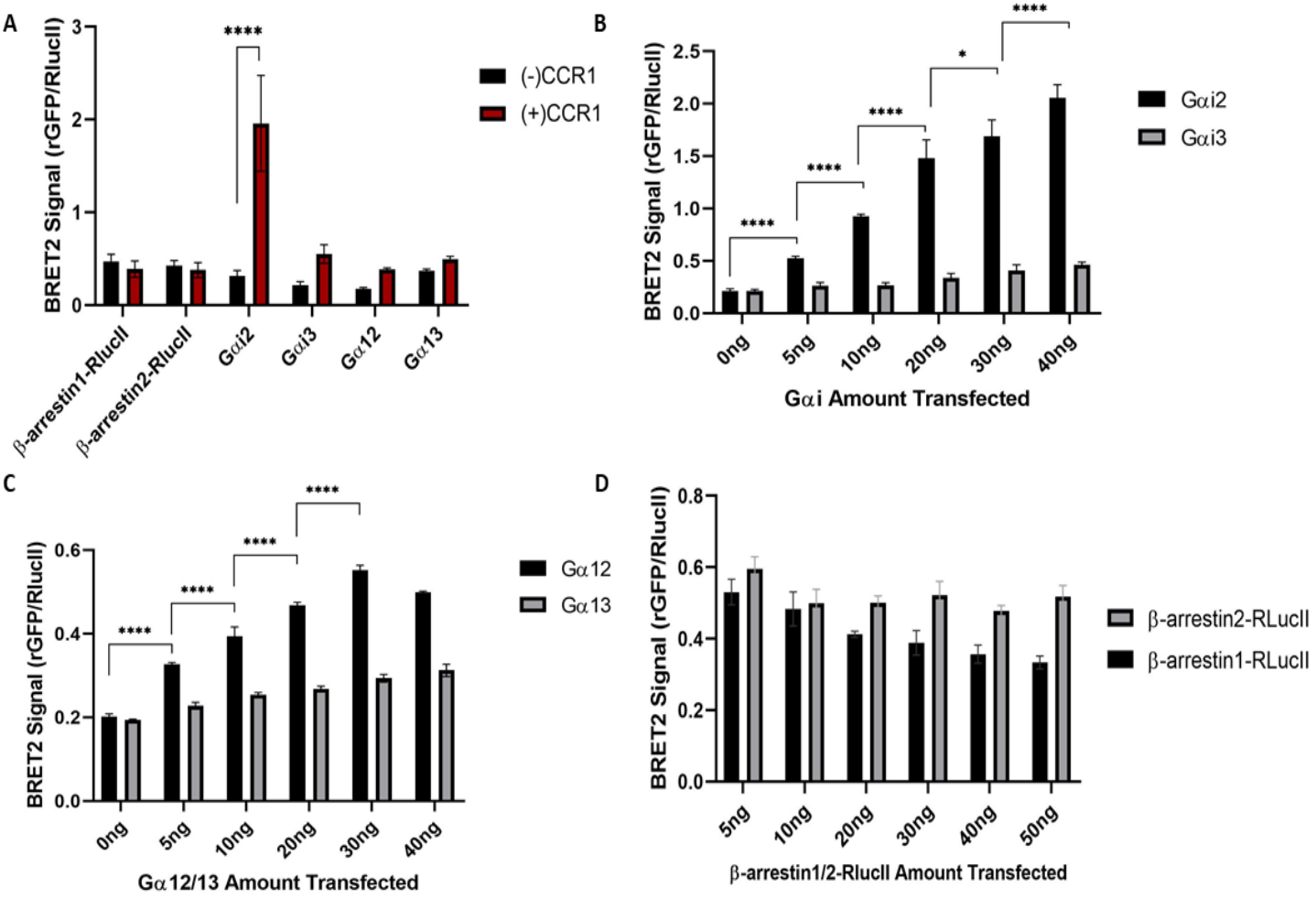

Figure 15. – CCR1 constitutive activity.

(A) HEK293 cells were transfected with the different EMTA biosensors, rGFP-CAAX, and the corresponding Gα subunits along with or without CCR1. **(B)** HEK293 cells were transfected with Rap1GAP-RlucII, rGFP-CAAX, CCR1 along with increasing amounts of Gαi2 or Gαi3 subunits. **(C)** HEK293 cells were transfected with PDZ-RhoGEF-RlucII, rGFP-CAAX, CCR1 along with increasing amounts of Gα12 or Gα13 subunits. **(D)** HEK293 cells were transfected with rGFP-CAAX and CCR1 along with increasing amounts of β-arrestin1-RlucII or β-arrestin2-RlucII. Cells were incubated for 2hrs in HBSS without any agonist stimulation. Raw BRET ratios are means ± s.e.m of at least two independent experiments plotted using GraphPad Prism® (GraphPad Software). The statistical significance was calculated using two-way ANOVA with Tuckey's post-test. *, $p < 0.05$; ****, $p < 0.0001$.

To further highlight the constitutive activity of CCR1, we proceeded to transfect HEK293 cells with the different EMTA biosensors, CCR1, and increasing amounts of Gα subunits or β-arrestin effectors. If there is indeed basal activation through CCR1, as we augment the expression of the signaling effector of choice, we should see a corresponding increase in the BRET2 signal

(fig 15B, C, D). These assays showed that when we increased the amount of Gαi2 subunit transfected, a significant increase in the BRET2 signal was observed. Conversely, increasing the expression of the Gαi3 subunit did not cause the same significant effect (fig 15B). Additionally, as we increased the expression of the Gα12 subunit, a significant increase in the BRET2 signal was observed, albeit at a lower level than the one observed in the Gαi2 subunit assay. On the other hand, the increased expression of Gα13 subunit did not result in any significant BRET2 signal surge (fig 15C). Finally, the increase of β-arrestin1/2-RlucII expression did not cause any rise in the BRET2 signal (fig 15D).

3.4. Testing CCL23/CCR1 axis signaling effects on the MAPK pathway.

3.4.1. Investigating CCL23/CCR1 axis signaling effects on the activation of ERK1/2 in AML and HEK293 cells.

After underlining the main downstream effectors that the CCL23/CCR1 axis can activate, we wanted to see the effects of CCL23/CCR1 on the MAPK pathway since it is known that this kinase cascade is highly involved in promoting cell growth and proliferation[105]. To do so, we choose to investigate different KM2A translocated AML cell lines, including Thp-1, Monomac-1, Nomo-1 because they showed high expression levels of CCR1. As a negative control, we selected the AML cell line KG-1a since CCR1 expression is essentially undetectable in these cells (fig 16A). After the selection, we serum-starved the cells and treated them with CCL23 for increasing periods of time. Then we extracted the protein and performed western blot assays blotting against phosphorylated Extracellular Signal-Regulated Kinase1 and 2 (p-ERK1/2) which is the activated form of the kinase ERK1/2, the ultimate kinase in the MAPK cascade[105]. We also blotted against ERK1/2 and GAPDH as loading controls (fig 16B). In addition to the AML cell lines, we treated serum-starved HEK293 cells, either overexpressing CCR1 or not, with CCL23 for increasing periods of time and performed similar western blot assays blotting against p-ERK1/2. We also blotted against ERK1/2 as a loading control (fig 16C).

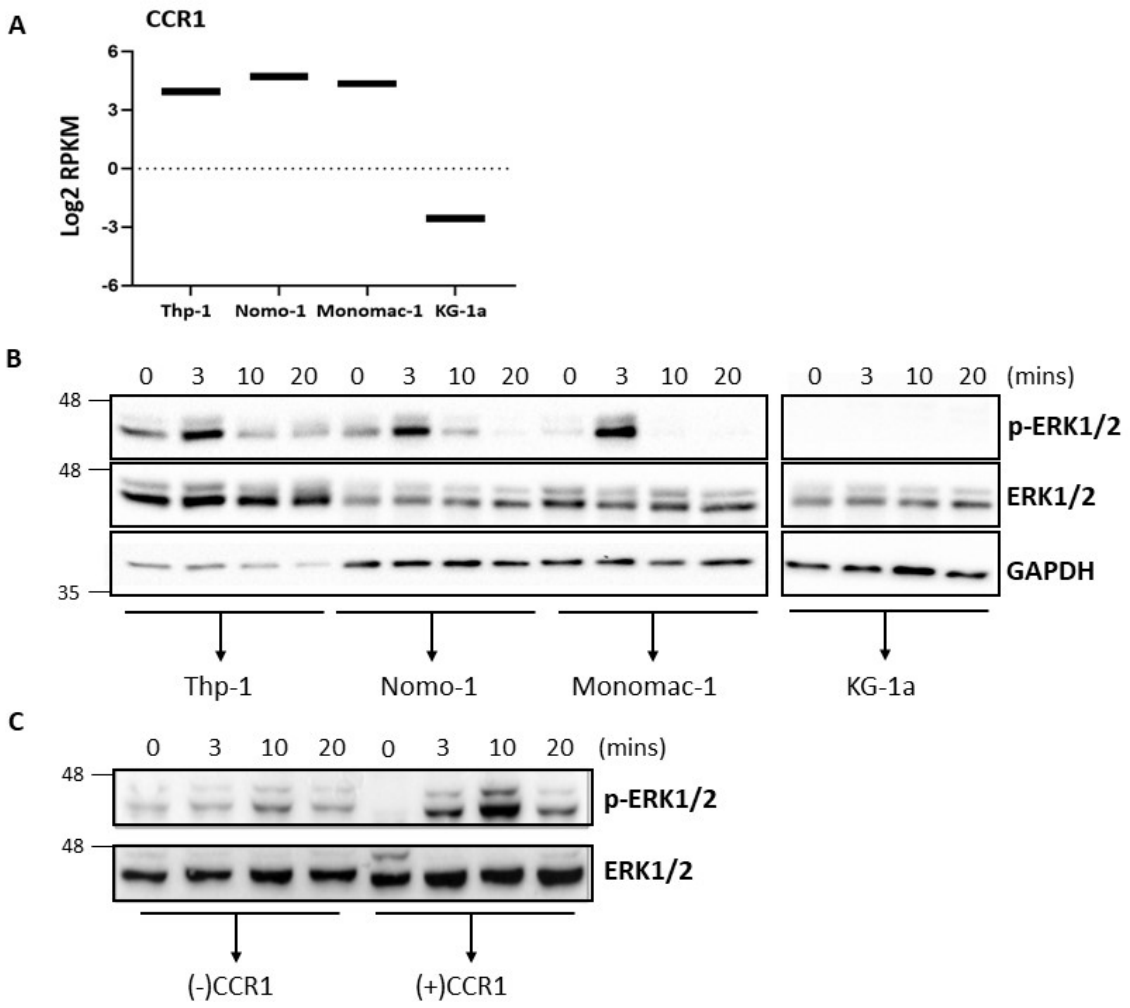

Figure 16. – Western blots of ERK1/2 phosphorylation in AML and HEK293 cells after CCL23 stimulation.

(A) Gene expression (log2 RPKM) of *CCR1* in Thp-1, Nomo-1, Monomac-1, and KG-1a cells. Dashed horizontal line represents the threshold for a gene to be considered expressed. Adapted from Barabe *et al.*[16] **(B)** The selected AML cell lines were serum-starved for 16hrs. Cells were incubated for the designated periods of time at 37ºC in the presence of CCL23 (100nM) and were immediately lysed. Western blots in the lysates were performed against p-ERK1/2, ERK1/2, and GAPDH (n=1). **(C)** HEK293 cells were either transfected with CCR1 or not and serum- starved for 16 hrs. Cells were incubated for the designated periods of time at 37ºC in the presence of CCL23 (100nM) and were immediately lysed. Western blots in the lysates were performed against p-ERK1/2 and ERK1/2 (n=2). Blots were developed and visualized using Image Lab software (Bio Rad®).

From the western blots we observed that CCL23 stimulation in Thp-1, Nomo-1, and Monomac-1 caused an increase in ERK1/2 phosphorylation after 3 mins of CCL23 stimulation as evident by the increase in the p-ERK1/2 band intensity when compared to 0 mins of CCL23 stimulation. On the other hand, CCL23 stimulation in KG-1a caused no increase in the ERK1/2

phosphorylation (fig 16B)[i]. Similarly, HEK293 cells expressing CCR1 showed an increase in the phosphorylation of ERK1/2 upon CCL23 stimulation with a peak intensity at the 10min stimulation mark. HEK293 devoid of CCR1 expression showed virtually no increase in p-ERK1/2 intensity (fig 16C).

3.4.2 Investigating CCL23/CCR1 axis signaling effects on the activation of ERK1/2 in HEK293 cells deleted for β-arrestin1/2.

Because our BRET assays indicated that CCL23/CCR1 signalling could cause a strong activation of β-arrestin1/2 biosensors, we wanted to test whether the phosphorylation of ERK1/2 post CCL23 treatment in HEK293 cells expressing CCR1 is mediated through β-arrestin1/2 pathways. To do so, we obtained HEK293 cells deleted for β-arrestin1 and β-arrestin2 proteins (HEK293-ArrKO), transfected them with (or without) CCR1 and/or β-arrestin1 and/or β-arrestin2, and stimulated the cells with CCL23 for different periods of time after serum-starvation. Then we performed a western blot assay blotting against CCR1, β-arrestin1/2, and p-ERK1/2. We also blotted against ERK1/2 and GAPDH as a loading control (fig 17).

[i] Refer to the Appendix section for biological replicates.

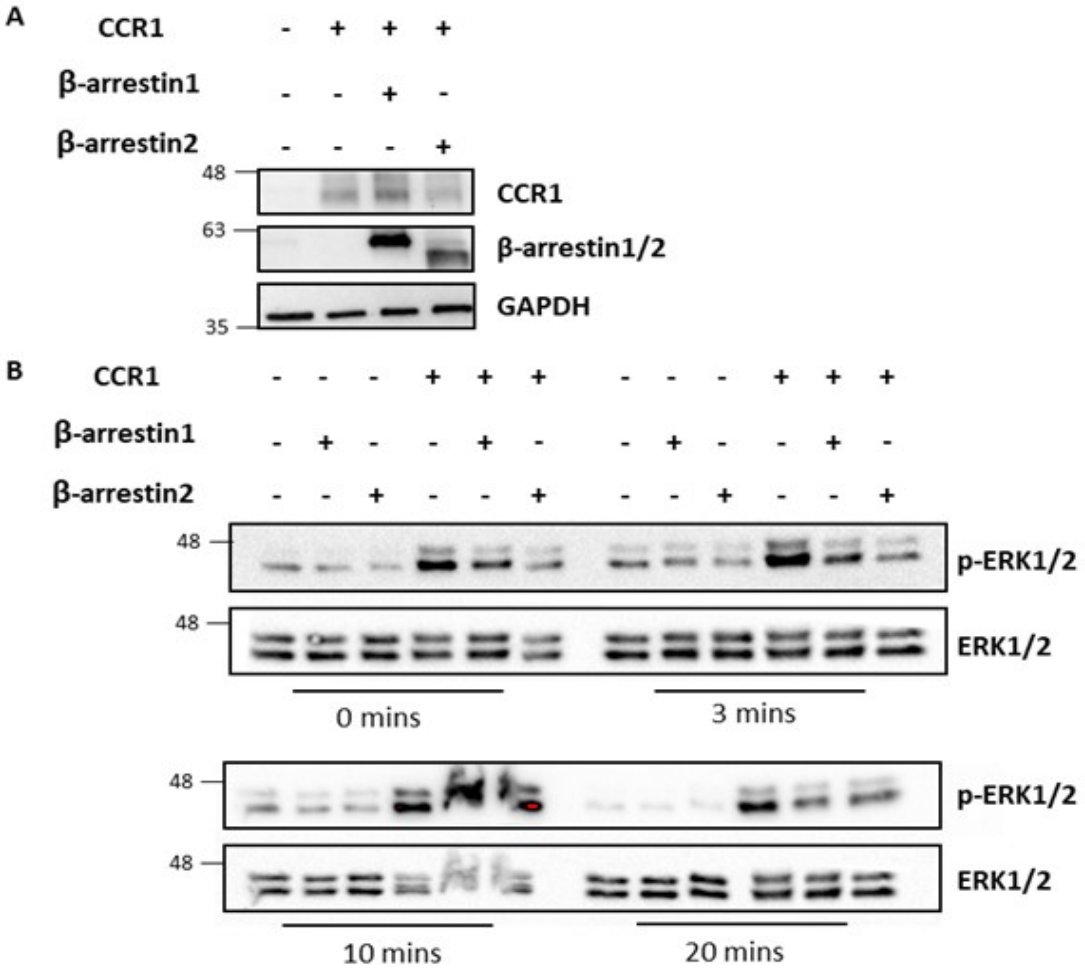
A
CCR1 - + + +
β-arrestin1 - - + -
β-arrestin2 - - - +
48
63
35
CCR1
β-arrestin1/2
GAPDH
B
CCR1 - - - + + + - - - + + +
β-arrestin1 - + - - + - - + - - + -
β-arrestin2 - - + - - + - - + - - +
48
48
p-ERK1/2
ERK1/2
0 mins
3 mins
48
48
p-ERK1/2
ERK1/2
10 mins
20 mins

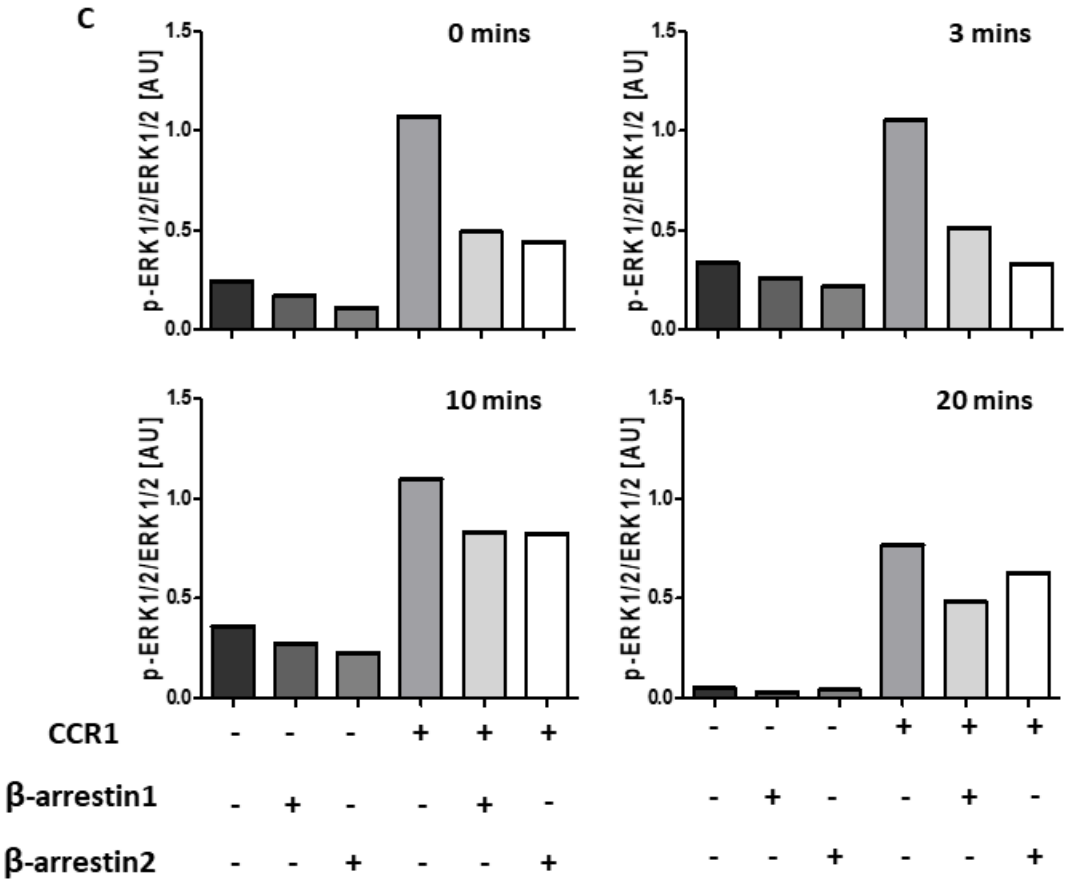
C
0 mins
3 mins
10 mins
20 mins
p-ERK1/2/ERK1/2 [AU]
1.5
1.0
0.5
0.0
CCR1
β-arrestin1
β-arrestin2

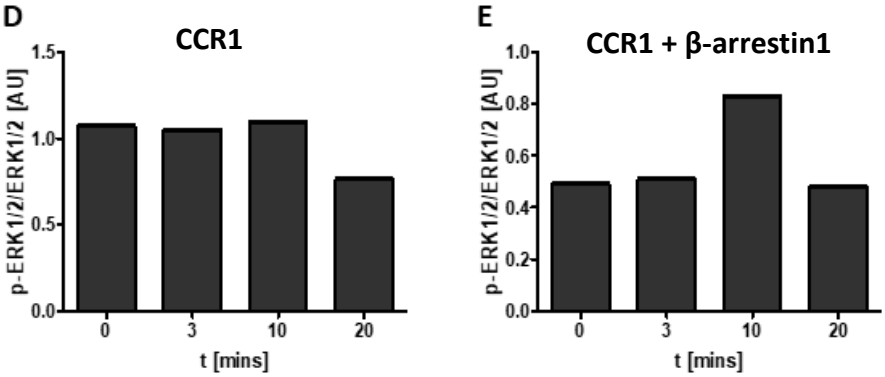
D
CCR1
E
CCR1 + β-arrestin1
p-ERK1/2/ERK1/2 [AU]
t [mins]
0
3
10
20

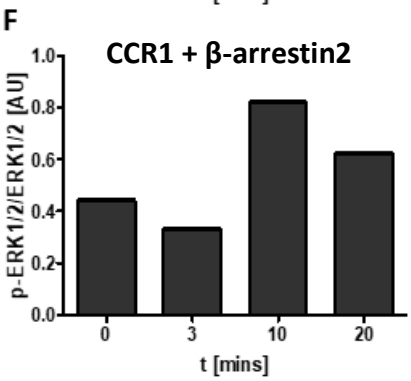
F
CCR1 + β-arrestin2
p-ERK1/2/ERK1/2 [AU]
t [mins]

Figure 17. – Western blots of ERK1/2 phosphorylation in HEK239-ArrKO cells after CCL23 stimulation.

(A) HEK293-ArrKO cells were transfected accordingly with the indicated proteins (CCR1, β-arrestin1, β-arrestin2) and serum-starved for 16 hrs and lysed. Western blots in the lysates were performed against CCR1 and β-arrestin1/2 (n=1). **(B)** HEK293-ArrKO cells were transfected accordingly with the indicated proteins (CCR1, β-arrestin1, β-arrestin2) and serum-starved for 16 hrs. Cells were incubated for the designated periods of time at 37°C in the presence of CCL23 (100nM) and were immediately lysed. Western blots in the lysates were performed against p-ERK1/2 and ERK1/2 (n=1). Blots were developed and visualized using Image Lab® (Bio Rad Software). **(C)** The densitometry of each band in the blot was measured using ImageJ® (National Institutes of Health Software). The densitometry ratios (p-ERK1/2 / ERK1/2) of each condition were calculated and plotted using GraphPad Prism® (GraphPad Software). **(D)** The densitometry ratios obtained from HEK293-ArrKO cells expressing CCR1 or **(E)** CCR1 and β-arrestin1 or **(F)** CCR1 and β-arrestin2 were plotted as a function of CCL23 stimulation times using GraphPad Prism® (GraphPad Software)

The western blot in (fig 17A) showed successful transfection of HEK293-ArrKO with CCR1, β-arrestin1, and β-arrestin2 as evident by the increase in the band intensities when compared to HEK293-ArrKO cells transfected with an empty vector. Also, it shows that a relatively equal amounts of the CCR1 proteins were expressed in all the cells. Moreover, the western blots against p-ERK1/2 and ERK1/2 and their corresponding semi-quantitative analysis revealed that, regardless of CCL23 stimulation, CCR1 expression in HEK-ArrKO cells caused an increase in phosphorylation of ERK1/2, evident by the increase in band intensities and densitometry ratios when compared to cells devoid of the CCR1 expression (fig 17B, C)[ii]. However, β-arrestin1 or β-arrestin2 overexpression along with CCR1 caused an apparent decrease in the phosphorylation of ERK1/2 when compared to conditions with CCR1 overexpression alone (fig 17B, C). When comparing the semi-quantitative densitometry ratios (p-ERK1/2/ ERK1/2) obtained from HEK293-ArrKO cells expressing CCR1 and β-arrestin1 (fig 17E) or CCR1 and β-arrestin2 (fig 17F) as a function of time of CCL23 treatment, we observed an increase in the phosphorylation of ERK1/2 at 10 mins of CCL23 stimulation as evident by an increase in the densitometry ratio when compared to the 0 mins of CCL23 stimulation. No such increase in the densitometry ratio was observed cells expressing CCR1 alone (fig 17D).

[ii] Due to COVID-19 complications, biological replicates were not obtained.

Chapter 4. Discussion

4.1. The EMTA and GRK2 biosensors are valid and can be used for efficient analysis of G protein coupling and β-arrestin recruitment.

This study highlights the efficient ability of the EMTA and GRK2 biosensors in detecting the coupling or recruitment of different G proteins and β-arrestin effectors. These biosensors provide several advantages in comparison to other protein-protein interaction and GPCR signaling detection methods. First, the GPCR and the Gα subunits in these biosensors are expressed in their native confirmation, devoid of any sort of tagging, contrary to a lot of other assays, such as β-gal complementation[106], PRESTO-Tango[107], or TGF-α shedding assays[108]. Having an unmodified GPCR is vital to avoid alteration of the intrinsic signaling responses. This is underlined in (fig 10A) as the EMTA biosensor was able to detect the activation of endogenous Gi proteins without the overexpression of any Gαi subunits. Second, these biosensors permit a real-time detection of the activation of the immediate downstream effector of GPCR. Many other assays rely on the detection of second messengers (i.e. cAMP)[109,110] or the activation of reporter genes (i.e. CRE, SRE)[111] which are situated further downstream in the signaling pathway, therefore, susceptible to cross-talk between different signaling pathways leading to difficulty in interpretation of the results.

Additionally, this study provides a head-to-head comparison between two eBRET2 biosensor (GRK2 and EMTA) and reveals that the newly described EMTA biosensor configuration might provide a better detection sensitivity. This is highlighted by the superior statistical significance of the EMTA biosensor in detecting the Gαi2 coupling after Dopamine stimulation (fig 10A) than the GRK2 biosensor (fig 10E). This could be due to the fact that the GRK2 biosensor requires the modification of core signaling components such as the GRK2 kinases and Gβγ subunits which, as mentioned earlier, could alter the intrinsic cellular signaling. Another reason could be that the configuration of the EMTA biosensor necessitates the BRET energy acceptor to be attached at the PM allowing for a better luminescence transmission than the energy acceptor of the GRK2 biosensor which is situated in the cytoplasm.

A potential caveat of these sensors is linked to the use of common effectors for all members of a given G protein subtype family and not individual biosensors for each G protein subtype. It cannot be excluded that different members of a given subtype family may display different relative affinities for their common effector.

4.2. CCL23/CCR1 axis signaling activates Gi2, G12/13, and β-arrestin1/2 albeit with a biased towards the β-arrestin1/2 recruitment.

By utilizing the eBRET2 biosensors, the first part of this project offers a comprehensive description of the CCL23 chemokine signaling network through the CCR1 receptor. Our results showed that CCL23/CCR1 axis activates the Gi family of proteins (fig 13A). This observation is not surprising since it has already been established that most chemokine receptors couple to Gαi proteins[70]. In addition, CCL23/CCR1 signaling has been shown to induce chemotaxis and increase the expression of other chemokines via signaling of the Gαi family[112]. Therefore, the CCL23/CCR1 signaling through Gi elucidate intercellular responses that could potentially enable the AML cells to metastasize. Nevertheless, our study reveals that there is a differential coupling within the members of the Gαi family as CCL23/CCR1 signaling showed a significant better efficacy towards Gαi2 coupling in contrast to Gαi3 coupling (table 3, fig 13A). This selectivity of a given GPCR for a specific member within one G protein family has been described before for other CC motif chemokine receptors such as CCR2, CCR5, and CCR7[99,113], but it has never been detected for the CCR1 receptor. Future work needs to be done to fully elucidate the functional consequences of this phenomenon. Moreover, by comparing the potencies and efficacies of CCL23/CCR1 axis signaling to the CCL3/CCR1 and CCL5/CCR1 axes, our results show that, although all three ligands exhibits similar efficacy, CCL23 is less potent than CCL3 and CCL5 for Gαi2 coupling (table 4, fig 14A).

Our experiments have also revealed that the CCL23/CCR1 axis activates the Gα12/13 families of G protein with a slight increase in efficacy for Gα13 protein coupling than Gα12 protein (table 3, fig13B). Previous reports have shown that other CC motif chemokines receptors such as CCR2 and CCR5 can activate Gα12 but not Gα13, whereas CCR7 cannot activate the Gα12/G13 family of protein at all[113]. Thus, our results present CCR1 as one of the unique CC motif chemokine receptors activating both Gα12 and Gα13 proteins. This is important because Gα12/13, also known as gep proto-oncogenes, are often overexpressed in cancers, including breast[114], prostate[115], and liver[116] cancers and plays a role in cell mobility, growth, differentiation, and transcription[117]. Hence, the CCL23/CCR1 signaling through G12/13 could possibly provide major advantages for AML development. Moreover, our comparison between the signaling of CCL23, CCL3, and

CCL5/CCR1 axes demonstrates that CCL23 has analogous potencies but reduced efficacies than CCL3 and CCL5 when activating Gα12 and Gα13, respectively (table 4, fig 14B, C).

This study also shows that none of the other two G protein families, Gαq and Gαs, are activated through the CCL23/CCR1 signaling (fig 11). These results agree with previously published data since several studies has shown that CCR1 can only couple to the Gαq family of proteins when it is activated by specific chemokines such as CCL3, CCL5, and CCL15 but not CCL9. This means that there CCR1 exhibit a ligand bias when stimulating Gαq and that CCL23, just like CCL9, might not be able to stimulate Gαq[118,119]. In addition, no studies to date has shown the ability of CCR1 or any other CC chemokine receptor to couple and activate the Gαs family of proteins. Nonetheless, it is important to note that while assessing the activation of Gαq and Gαs proteins our experiments were restricted to the less sensitive GRK2 biosensor.

Concerning the β-arrestin1/2 recruitment, established literature has described CCR1 to be able to selectively recruit β-arrestin2 but not β-arrestin1 when stimulated with CCL14[71]. By virtue of the EMTA biosensors, our findings illustrate that CCL23/CCR1 axis signaling can recruit both the β-arrestin1 and the β-arrestin2 effectors with parallel efficacies and potencies (table 3, fig 13C). By contrasting all the intermolecular downstream effectors that the CCL23/CCR1 axis signaling can activates, we observe that the CCL23 simulation recruits the β-arrestins effectors with higher relative potencies than the G-protein effectors (table 3). In addition, a comparison of the relative potencies between CCL23, CCL3, and CCL5 signaling through CCR1 shows that CCL23 is a more potent ligand than the other two for recruiting the β-arresin1/2 effectors (table 4). Altogether these results suggest that the CCL23/CCR1 axis demonstrate a bias towards a β-arrestin-dependent signaling pathway. β-arrestins were first thought to only regulate GPCRs desensitization and internalization after ligand binding[120]. It was found two decades ago that rather than only acting to terminate the GPCR stimulation, β-arrestins can also act as second messengers forming a multimeric complex with the GPCR to activate the MAPK cascade in a G protein-independent manner[121]. This is significant since the MAPK signaling cascade activates a vast array of downstream cellular responses vital for cell proliferation and growth suggesting that the AML cells could utilize the CCL23/CCR1/β-arrestin signaling pathway to insure the disease progression.

4.3. CCR1 is constitutively active which leads to G protein mediated signaling

In addition to describing the detailed signaling profile of the CCL23 chemokine, our project draws attention to the ability of the CCR1 receptor to be activated constitutively. A previous study, also using a BRET-based approach, reported that CCR1 exhibits a basal activity which can couple to Gi and recruit β-arrestin2 without the stimulation of any agonist[71]. In agreement with this study, our results show that CCR1 is indeed active constitutively and can couple to the Gαi family of proteins (fig 15A, B). Yet, our findings reveal that this constitutive activity can couple Gαi2 but not Gαi3 emphasizing once again the selectivity that the CCR1 receptor demonstrates for the different members of the Gαi family of proteins (fig 15B). Moreover, our study shows that CCR1 might also be able to couple and activate Gα12 constitutively (fig 15C), albeit with reduced efficacy relative to Gαi2. Contrary to the previous report, however, our eBRET2 assays does not indicate any direct recruitment of neither β-arrestin1 nor β-arrestin2 without some sort of ligand stimulation of CCR1 (fig 15D). The exact reason for the discrepancy between our results and those of Gilliland et al.[71] is unclear but may be linked to the BRET1 version used in their study where the BRET energy acceptor, YFP, is fused to the C-terminus of CCR1. This fusion can possibly alter the receptor's conformation and induces different signaling responses than the native CCR1 receptor used in all our eBRET2 assays. Another reason may be the different expression system used between their BRET assays and ours. While Gilliland et al.[71] used HEK293T, all our eBRET2 assays were done in HEK293SL cells which are a subclone derived from regular HEK293 cells that have a cobblestone appearance, and show better adherence as compared with HEK293T cells[89]. It should thus be kept in mind that the nature of the cells used to monitor receptor signaling could potentially impact the BRET assays and result in different outcomes.

Altogether, ours results indicates a constitutive activity of CCR1 which initiates a signal transduction through a G-protein mediated pathway mainly via coupling to the Gαi2 protein and probably, to a lesser extent, via Gα12 activation.

4.4. The CCL23/CCR1 axis signaling activates the MAPK pathway by phosphorylating ERK1/2 possibly through a β-arrestin1/2 mediated pathway.

Our BRET assays demonstrated a CCL23/CCR1 signaling bias towards the β-arrestin recruitment. As mentioned earlier, the β-arrestins can act as scaffolding proteins to activate the MAPK cascade. Therefore, in the second part of this project we demonstrate the effect of CCL23/CCR1 axis signaling on the MAPK cascade. We show that in KM3 bearing AML cell lines expressing the CCR1 receptor, CCL23 stimulation causes a relatively fast activation of ERK1/2 kinase (fig 16B). The same effects are seen in HEK293 cells expressing the CCR1 receptor, though requiring longer CCL23 stimulation times than the AML cell lines to cause a significant ERK1/2 activation (fig 16C). Both these results provide evidence that the CCL23/CCR1 axis signaling activates the MAPK cascade by phosphorylating the ERK1/2 kinase. This is supported by a recent study where the human CCL23 chemokine stimulation of bovine epithelial cells caused an increase ERK1/2 activation[122].

In this study we also try to pinpoint the downstream effector that the CCL23/CCR1 axis utilize to activate ERK1/2. Interestingly, we show that CCR1 expression in HEK293 cells deleted for β-arresins (HEK293-ArrKO) caused an increase in the phosphorylation of the ERK1/2 kinase without any stimulation of CCL23 (fig 17A, B). This increase in activation can be attributed to the CCR1 constitutive activity which can couple to Gαi2 and Gα12 proteins as revealed by our BRET assays. Many reports has shown that Gαi2 and Gα12 can activate the MAPK cascade explaining the evident increase in the ERK1/2 phosphorylation[123-125]. However, we do not see a similar phosphorylation of ERK1/2 in CCR1 expressing wild-type HEK293 cells without a stimulation from CCL23 (fig 16C). This could be explained by the fact that wild-type HEK293 cells ubiquitously express β-arrestin1/2 which can desensitize CCR1 and hinder the receptor's constitutive activity. This hypothesis is further supported by the fact that the introduction of either β-arrestin1 or β-arrestin2 alongside CCR1 in HEK293-ArrKO cells causes an apparent decrease in the ERK1/2 phosphorylation. On the other hand, when focusing on the effects of CCL23 stimulation in HEK293-ArrKO, our results demonstrate that the increase in the phosphorylation of ERK1/2 by the CCL23/CCR1 signaling requires the expression of either β-arrestin1 or β-arrestin2

alongside CCR1 (fig 17E, F). However, CCL23 stimulation of HEK293-ArrKO cells expressing CCR1 alone cannot cause any additional increase in the phosphorylation of ERK1/2 (fig 17D).

Altogether, these findings demonstrate that the CCR1 constitutive activity is stimulatory and triggers ERK1/2 phosphorylation which, to our best of knowledge, has never been shown before. Additionally, our findings imply that β-arrestin1/2 proteins are needed to put a stop to the CCR1 constitutive activity. Finally, our results also suggest the novel concept that CCL23/CCR1 axis signaling is dependent on β-arrestin proteins to activate the ERK1/2 kinase.

4.5. Future Work.

This project had the objective of identifying the CCL23/CCR1 signaling network and understand its effects on the MAPK pathway. Using a BRET approach, we have successfully identified 3 families of intermolecular downstream effectors that the CCL23/CCR1 can activate as follows: Gαi, Gα12/13, and β-arrestin1/2. We were not able to detect any activation for the Gαq and Gαs effectors. It will be interesting to repeat the BRET assays using the sensitive EMTA biosensors to be able to draw a more precise conclusion about the Gαq and Gαs activation. Our results equally show that CCR1 possess a constitutive activity that can activate the Gαi2 and Gα12 effectors. It will be interesting to repeat the BRET assays while treating the cells with an inverse agonist of CCR1 to test whether we can reverse this activity and detect a decrease in the BRET signal. We also show that CCR1 constitutive activity stimulate ERK1/2. As future work, it will be compelling to repeat the western blots in HEK293-ArrKO expressing CCR1 and treated with pertussis toxin (PTX) which is a potent Gi protein inhibitor. This way we can draw further conclusions on the potential involvement of Gαi2 in the CCR1 constitutive activity. Lastly, we demonstrate that the signaling of the CCL23/CCR1 axis activates ERK1/2 through a β-arrestin dependent manner. It will be essential to repeat similar western blot experiments in HEK293-ArrKO while overexpressing both β-arrestin1 and β-arrestin2 at the same time along with CCR1 to see whether we see a synergistic increase in the ERK1/2 activation after CCL23 stimulation.

Chapter 5. Conclusion and Perspective

My masters project provides a novel biological characterization of the signaling network of the CCL23 chemokine and its corresponding receptor, CCR1, which are two highly upregulated proteins in the KMT2A-MLLT3 AML disease. Through our highly effective BRET sensors and immunoblots we demonstrated many novel concepts, such as the ability of CCL23/CCR1 axis to activate Gα12/G13 and β-arrestin1/2 in addition to selectively activating Gαi2 within the Gαi family. All these effectors can elucidate biological responses that could provide major benefits for the AML cells proliferation and metastasis. Another novel notion presented by our study is the selectivity of CCL23 for the activation of the β-arrestin1 and β-arrestin2 effectors, when compared to two other chemokines, CCL3 and CCL5, further asserting the extent of the biased agonism exhibited by the human chemokine-receptor network. The final novel theory provided by this project is the notion that CCL23/CCR1 axis signaling utilizes a β-arrestin-dependent pathway to activate the ERK1/2 kinase.

Now that we understand the signaling of the CCL23 chemokine, the question to be answered remains: What are the effects of the CCL23/CCR1 signaling in the context of KM3 AML?

A lot of work still needs to be accomplished to answer that question. Therefore, future efforts should focus on understanding the essentiality of CCL23, CCR1, and the MAPK cascade to the KM3 AML cells. In addition, careful studies should be done to test the phenotypic and the genotypic consequences of CCL23 signaling in the KM3 AML cells in comparison to normal stem cells.

By clarifying this, it will allow us to rationally design new inhibitors against CCL23 or the proteins that transmit the signal through the cell. This will ultimately provide new types of therapy for patients. This is significant because current leukemia treatments are highly inconsistent[126], so the development of novel effective and targeted treatments for patients would have a substantial clinical impact.

Chapter 6. Appendix

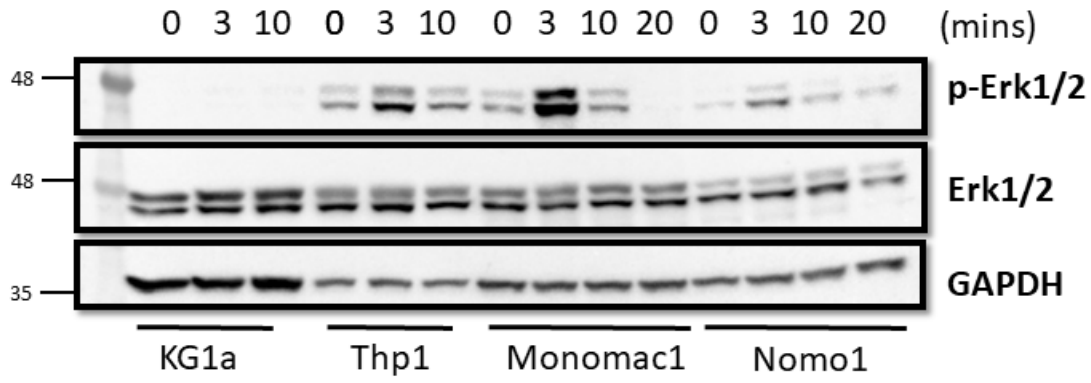

Figure 18. – Replicates of Western blots for ERK1/2 Phosphorylation in AML cells after CCL23 stimulation.

The selected AML cell lines were serum-starved for 16hrs. Cells were incubated for the designated periods of time at 37°C in the presence of CCL23 (100nM) and were immediately lysed. Western blots in the lysates were performed against p-ERK1/2, ERK1/2, and GAPDH

Chapter 7. References

1. Rieger MA, Schroeder T. Hematopoiesis. *Cold Spring Harb Perspect Biol.* 2012;4(12).
2. Jagannathan-Bogdan M, Zon LI. Hematopoiesis. *Development.* 2013;140(12):2463-2467.
3. Juliusson G, Hough R. Leukemia. *Prog Tumor Res.* 2016;43:87-100.
4. De Kouchkovsky I, Abdul-Hay M. 'Acute myeloid leukemia: a comprehensive review and 2016 update'. *Blood Cancer J.* 2016;6(7):e441.
5. Dohner H, Estey EH, Amadori S, et al. Diagnosis and management of acute myeloid leukemia in adults: recommendations from an international expert panel, on behalf of the European LeukemiaNet. *Blood.* 2010;115(3):453-474.
6. Appelbaum FR, Gundacker H, Head DR, et al. Age and acute myeloid leukemia. *Blood.* 2006;107(9):3481-3485.
7. Juliusson G, Antunovic P, Derolf A, et al. Age and acute myeloid leukemia: real world data on decision to treat and outcomes from the Swedish Acute Leukemia Registry. *Blood.* 2009;113(18):4179-4187.
8. Steliarova-Foucher E, Colombet M, Ries LAG, et al. International incidence of childhood cancer, 2001-10: a population-based registry study. *Lancet Oncol.* 2017;18(6):719-731.
9. Lindsley RC, Mar BG, Mazzola E, et al. Acute myeloid leukemia ontogeny is defined by distinct somatic mutations. *Blood.* 2015;125(9):1367-1376.
10. Kihara R, Nagata Y, Kiyoi H, et al. Comprehensive analysis of genetic alterations and their prognostic impacts in adult acute myeloid leukemia patients. *Leukemia.* 2014;28(8):1586-1595.
11. Byrd JC, Mrózek K, Dodge RK, et al. Pretreatment cytogenetic abnormalities are predictive of induction success, cumulative incidence of relapse, and overall survival in adult patients with de novo acute myeloid leukemia: results from Cancer and Leukemia Group B (CALGB 8461): Presented in part at the 43rd annual meeting of the American Society of Hematology, Orlando, FL, December 10, 2001, and published in abstract form.59. *Blood.* 2002;100(13):4325-4336.
12. Balgobind BV, Raimondi SC, Harbott J, et al. Novel prognostic subgroups in childhood 11q23/MLL-rearranged acute myeloid leukemia: results of an international retrospective study. *Blood.* 2009;114(12):2489-2496.
13. Downing JR, Shannon KM. Acute leukemia: a pediatric perspective. *Cancer Cell.* 2002;2(6):437-445.
14. Meyer C, Burmeister T, Groger D, et al. The MLL recombinome of acute leukemias in 2017. *Leukemia.* 2018;32(2):273-284.
15. Shih AH, Abdel-Wahab O, Patel JP, Levine RL. The role of mutations in epigenetic regulators in myeloid malignancies. *Nature Reviews Cancer.* 2012;12(9):599-612.
16. Barabe F, Gil L, Celton M, et al. Modeling human MLL-AF9 translocated acute myeloid leukemia from single donors reveals RET as a potential therapeutic target. *Leukemia.* 2017;31(5):1166-1176.
17. Marschalek R. Mixed lineage leukemia: roles in human malignancies and potential therapy. *Febs j.* 2010;277(8):1822-1831.
18. Garcia-Alai MM, Allen MD, Joerger AC, Bycroft M. The structure of the FYR domain of transforming growth factor beta regulator 1. *Protein Sci.* 2010;19(7):1432-1438.
19. Wang P, Lin C, Smith ER, et al. Global analysis of H3K4 methylation defines MLL family member targets and points to a role for MLL1-mediated H3K4 methylation in the regulation of transcriptional initiation by RNA polymerase II. *Mol Cell Biol.* 2009;29(22):6074-6085.

20. Muntean AG, Tan J, Sitwala K, et al. The PAF complex synergizes with MLL fusion proteins at HOX loci to promote leukemogenesis. *Cancer Cell.* 2010;17(6):609-621.
21. Yokoyama A, Cleary ML. Menin critically links MLL proteins with LEDGF on cancer-associated target genes. *Cancer Cell.* 2008;14(1):36-46.
22. Zeleznik-Le NJ, Harden AM, Rowley JD. 11q23 translocations split the "AT-hook" cruciform DNA-binding region and the transcriptional repression domain from the activation domain of the mixed-lineage leukemia (MLL) gene. *Proc Natl Acad Sci U S A.* 1994;91(22):10610-10614.
23. Fair K, Anderson M, Bulanova E, Mi H, Tropschug M, Diaz MO. Protein interactions of the MLL PHD fingers modulate MLL target gene regulation in human cells. *Mol Cell Biol.* 2001;21(10):3589-3597.
24. Ali M, Hom RA, Blakeslee W, Ikenouye L, Kutateladze TG. Diverse functions of PHD fingers of the MLL/KMT2 subfamily. *Biochim Biophys Acta.* 2014;1843(2):366-371.
25. Krivtsov AV, Armstrong SA. MLL translocations, histone modifications and leukaemia stem-cell development. *Nat Rev Cancer.* 2007;7(11):823-833.
26. Rao RC, Dou Y. Hijacked in cancer: the KMT2 (MLL) family of methyltransferases. *Nat Rev Cancer.* 2015;15(6):334-346.
27. Paggetti J, Largeot A, Aucagne R, et al. Crosstalk between leukemia-associated proteins MOZ and MLL regulates HOX gene expression in human cord blood CD34+ cells. *Oncogene.* 2010;29(36):5019-5031.
28. Li Y, Wen H, Xi Y, et al. AF9 YEATS domain links histone acetylation to DOT1L-mediated H3K79 methylation. *Cell.* 2014;159(3):558-571.
29. He N, Chan CK, Sobhian B, et al. Human Polymerase-Associated Factor complex (PAFc) connects the Super Elongation Complex (SEC) to RNA polymerase II on chromatin. *Proc Natl Acad Sci U S A.* 2011;108(36):E636-645.
30. Kuntimaddi A, Achille NJ, Thorpe J, et al. Degree of recruitment of DOT1L to MLL-AF9 defines level of H3K79 Di- and tri-methylation on target genes and transformation potential. *Cell Rep.* 2015;11(5):808-820.
31. Meyer C, Lopes BA, Caye-Eude A, et al. Human MLL/KMT2A gene exhibits a second breakpoint cluster region for recurrent MLL-USP2 fusions. *Leukemia.* 2019;33(9):2306-2340.
32. Li BE, Ernst P. Two decades of leukemia oncoprotein epistasis: the MLL1 paradigm for epigenetic deregulation in leukemia. *Exp Hematol.* 2014;42(12):995-1012.
33. Chan AKN, Chen CW. Rewiring the Epigenetic Networks in MLL-Rearranged Leukemias: Epigenetic Dysregulation and Pharmacological Interventions. *Front Cell Dev Biol.* 2019;7:81.
34. Slany RK. The molecular biology of mixed lineage leukemia. *Haematologica.* 2009;94(7):984-993.
35. Meyer C, Hofmann J, Burmeister T, et al. The MLL recombinome of acute leukemias in 2013. *Leukemia.* 2013;27(11):2165-2176.
36. Winters AC, Bernt KM. MLL-Rearranged Leukemias-An Update on Science and Clinical Approaches. *Front Pediatr.* 2017;5:4.
37. Wächter K, Kowarz E, Marschalek RJCl. Functional characterisation of different MLL fusion proteins by using inducible Sleeping Beauty vectors. 2014;352(2):196-202.
38. Marschalek RJBeBA-GRM. The reciprocal world of MLL fusions: A personal view. 2020:194547.

39. Tsuchiya S, Yamabe M, Yamaguchi Y, Kobayashi Y, Konno T, Tada K. Establishment and characterization of a human acute monocytic leukemia cell line (THP-1). *Int J Cancer.* 1980;26(2):171-176.
40. Matsuo Y, MacLeod RA, Uphoff CC, et al. Two acute monocytic leukemia (AML-M5a) cell lines (MOLM-13 and MOLM-14) with interclonal phenotypic heterogeneity showing MLL-AF9 fusion resulting from an occult chromosome insertion, ins(11;9)(q23;p22p23). *Leukemia.* 1997;11(9):1469-1477.
41. Milan T, Canaj H, Villeneuve C, et al. Pediatric leukemia: Moving toward more accurate models. *Exp Hematol.* 2019;74:1-12.
42. Corral J, Lavenir I, Impey H, et al. An Mll-AF9 fusion gene made by homologous recombination causes acute leukemia in chimeric mice: a method to create fusion oncogenes. *Cell.* 1996;85(6):853-861.
43. Barabe F, Kennedy JA, Hope KJ, Dick JE. Modeling the initiation and progression of human acute leukemia in mice. *Science.* 2007;316(5824):600-604.
44. Fernandez EJ, Lolis E. Structure, function, and inhibition of chemokines. *Annu Rev Pharmacol Toxicol.* 2002;42:469-499.
45. Viola A, Luster AD. Chemokines and their receptors: drug targets in immunity and inflammation. *Annu Rev Pharmacol Toxicol.* 2008;48:171-197.
46. Gerard C, Rollins BJ. Chemokines and disease. *Nature Immunology.* 2001;2(2):108-115.
47. Zlotnik A, Yoshie O. Chemokines: a new classification system and their role in immunity. *Immunity.* 2000;12(2):121-127.
48. Stone MJ, Hayward JA, Huang C, Z EH, Sanchez J. Mechanisms of Regulation of the Chemokine-Receptor Network. *Int J Mol Sci.* 2017;18(2).
49. Patel VP, Kreider BL, Li Y, et al. Molecular and functional characterization of two novel human CC chemokines as inhibitors of two distinct classes of myeloid progenitors. 1997;185(7):1163-1172.
50. Miao Z, Premack BA, Wei Z, et al. Proinflammatory Proteases Liberate a Discrete High-Affinity Functional FPRL1 (CCR12) Ligand from CCL23. 2007;178(11):7395-7404.
51. Youn B-S, Zhang SM, Broxmeyer HE, et al. Characterization of CKβ8 and CKβ8-1: two alternatively spliced forms of human β-chemokine, chemoattractants for neutrophils, monocytes, and lymphocytes, and potent agonists at CC chemokine receptor 1. 1998;91(9):3118-3126.
52. Berahovich RD, Miao Z, Wang Y, Premack B, Howard MC, Schall TJJTJoI. Proteolytic activation of alternative CCR1 ligands in inflammation. 2005;174(11):7341-7351.
53. Hwang J, Son K-N, Kim CW, et al. Human CC chemokine CCL23, a ligand for CCR1, induces endothelial cell migration and promotes angiogenesis. *Cytokine.* 2005;30(5):254-263.
54. Votta BJ, White JR, Dodds RA, et al. CKβ-8 [CCL23], a novel CC chemokine, is chemotactic for human osteoclast precursors and is expressed in bone tissues. 2000;183(2):196-207.
55. Arruda-Silva F, Bianchetto-Aguilera F, Gasperini S, et al. Human Neutrophils Produce CCL23 in Response to Various TLR-Agonists and TNFα. 2017;7(176).
56. Matsumoto K, Fukuda S, Hashimoto N, Saito HJIaoa, immunology. Human eosinophils produce and release a novel chemokine, CCL23, in vitro. 2011;155(Suppl. 1):34-39.
57. Novak H, Müller A, Harrer N, Günther C, Carballido JM, Woisetschläger MJTJoI. CCL23 expression is induced by IL-4 in a STAT6-dependent fashion. 2007;178(7):4335-4341.

58. Poposki JA, Uzzaman A, Nagarkar DR, et al. Increased expression of the chemokine CCL23 in eosinophilic chronic rhinosinusitis with nasal polyps. *J Allergy Clin Immunol.* 2011;128(1):73-81.e74.
59. Yanaba K, Yoshizaki A, Muroi E, et al. Serum CCL23 levels are increased in patients with systemic sclerosis. 2011;303(1):29-34.
60. Celik H, Lindblad KE, Popescu B, et al. A Novel Proteomic Profiling of the Bone Marrow Microenvironment Reveals Elevated Levels of the Chemokine CCL23 Isoforms in Acute Myeloid Leukemia. *Blood.* 2019;134(Supplement_1):2709-2709.
61. Chemokine/chemokine receptor nomenclature. *Cytokine.* 2003;21(1):48-49.
62. Bennett LD, Fox JM, Signoret N. Mechanisms regulating chemokine receptor activity. *Immunology.* 2011;134(3):246-256.
63. Shoichet BK, Kobilka BKJTips. Structure-based drug screening for G-protein-coupled receptors. 2012;33(5):268-272.
64. Cabrera-Vera TM, Vanhauwe J, Thomas TO, et al. Insights into G protein structure, function, and regulation. 2003;24(6):765-781.
65. Downes G, Gautam NJG. The G protein subunit gene families. 1999;62(3):544-552.
66. Peterson YK, Luttrell LM. The Diverse Roles of Arrestin Scaffolds in G Protein-Coupled Receptor Signaling. *Pharmacol Rev.* 2017;69(3):256-297.
67. Rajagopal S, Bassoni DL, Campbell JJ, Gerard NP, Gerard C, Wehrman TS. Biased agonism as a mechanism for differential signaling by chemokine receptors. *J Biol Chem.* 2013;288(49):35039-35048.
68. Gao J-L, Kuhns DB, Tiffany HL, et al. Structure and functional expression of the human macrophage inflammatory protein 1 alpha/RANTES receptor. 1993;177(5):1421-1427.
69. Scholten DJ, Canals M, Maussang D, et al. Pharmacological modulation of chemokine receptor function. *Br J Pharmacol.* 2012;165(6):1617-1643.
70. Steen A, Larsen O, Thiele S, Rosenkilde MM. Biased and G Protein-Independent Signaling of Chemokine Receptors. 2014;5(277).
71. Gilliland CT, Salanga CL, Kawamura T, Trejo J, Handel TM. The chemokine receptor CCR1 is constitutively active, which leads to G protein-independent, β-arrestin-mediated internalization. *J Biol Chem.* 2013;288(45):32194-32210.
72. Murphy PM, Baggiolini M, Charo IF, et al. International union of pharmacology. XXII. Nomenclature for chemokine receptors. *Pharmacol Rev.* 2000;52(1):145-176.
73. Cheng SS, Lai JJ, Lukacs NW, Kunkel SL. Granulocyte-macrophage colony stimulating factor up-regulates CCR1 in human neutrophils. *J Immunol.* 2001;166(2):1178-1184.
74. Loetscher P, Moser B. Homing chemokines in rheumatoid arthritis. *Arthritis Res.* 2002;4(4):233-236.
75. Karpus WJ, Lukacs NW, McRae BL, Strieter RM, Kunkel SL, Miller SD. An important role for the chemokine macrophage inflammatory protein-1 alpha in the pathogenesis of the T cell-mediated autoimmune disease, experimental autoimmune encephalomyelitis. *J Immunol.* 1995;155(10):5003-5010.
76. Joubert P, Lajoie-Kadoch S, Welman M, et al. Expression and regulation of CCR1 by airway smooth muscle cells in asthma. *J Immunol.* 2008;180(2):1268-1275.
77. Halks-Miller M, Schroeder ML, Haroutunian V, et al. CCR1 is an early and specific marker of Alzheimer's disease. *Ann Neurol.* 2003;54(5):638-646.
78. Maiga A, Lemieux S, Pabst C, et al. Transcriptome analysis of G protein-coupled receptors in distinct genetic subgroups of acute myeloid leukemia: identification of potential disease-specific targets. *Blood Cancer J.* 2016;6(6):e431.

79. Xu Y, Piston DW, Johnson CH. A bioluminescence resonance energy transfer (BRET) system: application to interacting circadian clock proteins. *Proc Natl Acad Sci U S A.* 1999;96(1):151-156.
80. Bacart J, Corbel C, Jockers R, Bach S, Couturier C. The BRET technology and its application to screening assays. *Biotechnol J.* 2008;3(3):311-324.
81. Wu P, Brand L. Resonance energy transfer: methods and applications. *Anal Biochem.* 1994;218(1):1-13.
82. Shih WM, Gryczynski Z, Lakowicz JR, Spudich JA. A FRET-based sensor reveals large ATP hydrolysis-induced conformational changes and three distinct states of the molecular motor myosin. *Cell.* 2000;102(5):683-694.
83. Clegg RM, Murchie AI, Zechel A, Lilley DM. Observing the helical geometry of double-stranded DNA in solution by fluorescence resonance energy transfer. *Proc Natl Acad Sci U S A.* 1993;90(7):2994-2998.
84. Bertrand L, Parent S, Caron M, et al. The BRET2/arrestin assay in stable recombinant cells: a platform to screen for compounds that interact with G protein-coupled receptors (GPCRS). *J Recept Signal Transduct Res.* 2002;22(1-4):533-541.
85. Loening AM, Fenn TD, Wu AM, Gambhir SS. Consensus guided mutagenesis of Renilla luciferase yields enhanced stability and light output. *Protein Eng Des Sel.* 2006;19(9):391-400.
86. Dacres H, Michie M, Wang J, Pfleger KDG, Trowell SC. Effect of enhanced Renilla luciferase and fluorescent protein variants on the Förster distance of Bioluminescence resonance energy transfer (BRET). *Biochemical and Biophysical Research Communications.* 2012;425(3):625-629.
87. Fujii H, Noda K, Asami Y, Kuroda A, Sakata M, Tokida A. Increase in bioluminescence intensity of firefly luciferase using genetic modification. *Analytical Biochemistry.* 2007;366(2):131-136.
88. Arai R, Nakagawa H, Kitayama A, Ueda H, Nagamune T. Detection of protein-protein interaction by bioluminescence resonance energy transfer from firefly luciferase to red fluorescent protein. *Journal of Bioscience and Bioengineering.* 2002;94(4):362-364.
89. Namkung Y, Le Gouill C, Lukashova V, et al. Monitoring G protein-coupled receptor and β-arrestin trafficking in live cells using enhanced bystander BRET. *Nat Commun.* 2016;7:12178.
90. Lodowski DT, Pitcher JA, Capel WD, Lefkowitz RJ, Tesmer JJG. Keeping G Proteins at Bay: A Complex Between G Protein-Coupled Receptor Kinase 2 and Gßγ. 2003;300(5623):1256-1262.
91. Namkung Y, LeGouill C, Kumar S, et al. Functional selectivity profiling of the angiotensin II type 1 receptor using pathway-wide BRET signaling sensors. 2018;11(559).
92. Luttrell LM, Wang J, Plouffe B, et al. Manifold roles of β-arrestins in GPCR signaling elucidated with siRNA and CRISPR/Cas9. 2018;11(549):eaat7650.
93. Zimmerman B, Beautrait A, Aguila B, et al. Differential β-Arrestin–Dependent Conformational Signaling and Cellular Responses Revealed by Angiotensin Analogs. 2012;5(221):ra33-ra33.
94. Quoyer J, Janz JM, Luo J, et al. Pepducin targeting the CXC chemokine receptor type 4 acts as a biased agonist favoring activation of the inhibitory G protein. 2013;110(52):E5088-E5097.

95. Ehrlich AT, Semache M, Bailly J, et al. Mapping GPR88-Venus illuminates a novel role for GPR88 in sensory processing. *Brain Struct Funct.* 2018;223(3):1275-1296.
96. Parent JL, Labrecque P, Orsini MJ, Benovic JL. Internalization of the TXA2 receptor alpha and beta isoforms. Role of the differentially spliced cooh terminus in agonist-promoted receptor internalization. *J Biol Chem.* 1999;274(13):8941-8948.
97. Breton B, Sauvageau É, Zhou J, Bonin H, Le Gouill C, Bouvier M. Multiplexing of multicolor bioluminescence resonance energy transfer. *Biophys J.* 2010;99(12):4037-4046.
98. Breit A, Gagnidze K, Devi LA, Lagacé M, Bouvier M. Simultaneous Activation of the δ Opioid Receptor (δOR)/Sensory Neuron-Specific Receptor-4 (SNSR-4) Hetero-Oligomer by the Mixed Bivalent Agonist Bovine Adrenal Medulla Peptide 22 Activates SNSR-4 but Inhibits δOR Signaling. 2006;70(2):686-696.
99. Avet C, Mancini A, Breton B, et al. Selectivity Landscape of 100 Therapeutically Relevant GPCR Profiled by an Effector Translocation-Based BRET Platform. 2020:2020.2004.2020.052027.
100. McAvoy T, Zhou M-m, Greengard P, Nairn ACJPotNAoS. Phosphorylation of Rap1GAP, a striatally enriched protein, by protein kinase A controls Rap1 activity and dendritic spine morphology. 2009;106(9):3531-3536.
101. Missale C, Nash SR, Robinson SW, Jaber M, Caron MG. Dopamine receptors: from structure to function. *Physiol Rev.* 1998;78(1):189-225.
102. Honma S, Saika M, Ohkubo S, Kurose H, Nakahata N. Thromboxane A2 receptor-mediated G12/13-dependent glial morphological change. *Eur J Pharmacol.* 2006;545(2-3):100-108.
103. Bohn LM, Lefkowitz RJ, Gainetdinov RR, Peppel K, Caron MG, Lin FT. Enhanced morphine analgesia in mice lacking beta-arrestin 2. *Science.* 1999;286(5449):2495-2498.
104. Gautam D, Han SJ, Duttaroy A, et al. Role of the M3 muscarinic acetylcholine receptor in beta-cell function and glucose homeostasis. *Diabetes Obes Metab.* 2007;9 Suppl 2:158-169.
105. Meloche S, Pouysségur J. The ERK1/2 mitogen-activated protein kinase pathway as a master regulator of the G1- to S-phase transition. *Oncogene.* 2007;26(22):3227-3239.
106. Bassoni DL, Raab WJ, Achacoso PL, Loh CY, Wehrman TS. Measurements of β-arrestin recruitment to activated seven transmembrane receptors using enzyme complementation. *Methods Mol Biol.* 2012;897:181-203.
107. Kroeze WK, Sassano MF, Huang X-P, et al. PRESTO-Tango as an open-source resource for interrogation of the druggable human GPCRome. *Nature Structural & Molecular Biology.* 2015;22(5):362-369.
108. Inoue A, Raimondi F, Kadji FMN, et al. Illuminating G-protein-coupling selectivity of GPCRs. 2019;177(7):1933-1947. e1925.
109. Bradley J, McLoughlin D. Use of the DiscoveRx Hit hunter cAMPII assay for direct measurement of cAMP in Gs and Gi GPCRs. *Methods Mol Biol.* 2009;552:171-179.
110. Rajagopal S, Ahn S, Rominger DH, et al. Quantifying ligand bias at seven-transmembrane receptors. *Mol Pharmacol.* 2011;80(3):367-377.
111. Cheng Z, Garvin D, Paguio A, Stecha P, Wood K, Fan FJCcg. Luciferase reporter assay system for deciphering GPCR pathways. 2010;4:84.
112. Kim J, Kim YS, Ko JJLs. CKβ8/CCL23 induces cell migration via the Gi/Go protein/PLC/PKCδ/NF-κB and is involved in inflammatory responses. 2010;86(9-10):300-308.

113. Corbisier J, Galès C, Huszagh A, Parmentier M, Springael JY. Biased signaling at chemokine receptors. *J Biol Chem.* 2015;290(15):9542-9554.
114. Kelly P, Moeller BJ, Juneja J, et al. The G12 family of heterotrimeric G proteins promotes breast cancer invasion and metastasis. 2006;103(21):8173-8178.
115. Kelly P, Stemmle LN, Madden JF, Fields TA, Daaka Y, Casey PJJJoBC. A role for the G12 family of heterotrimeric G proteins in prostate cancer invasion. 2006;281(36):26483-26490.
116. Yang Y, Lee W, Lee C, et al. Gα 12 gep oncogene deregulation of p53-responsive microRNAs promotes epithelial–mesenchymal transition of hepatocellular carcinoma. 2015;34(22):2910-2921.
117. Yang YM, Kuen D-S, Chung Y, Kurose H, Kim SG. Gα12/13 signaling in metabolic diseases. *Experimental & Molecular Medicine.* 2020;52(6):896-910.
118. Tian Y, New DC, Yung LY, et al. Differential chemokine activation of CC chemokine receptor 1-regulated pathways: ligand selective activation of Galpha 14-coupled pathways. *Eur J Immunol.* 2004;34(3):785-795.
119. Lee MM, Wong YH. CCR1-mediated activation of Nuclear Factor-kappaB in THP-1 monocytic cells involves Pertussis Toxin-insensitive Galpha(14) and Galpha(16) signaling cascades. *J Leukoc Biol.* 2009;86(6):1319-1329.
120. Freedman NJ, Lefkowitz RJJRpihr. Desensitization of G protein-coupled receptors. 1996;51:319-351; discussion 352.
121. Luttrell L, Ferguson S, Daaka Y, et al. β-Arrestin-dependent formation of β2 adrenergic receptor-Src protein kinase complexes. 1999;283(5402):655-661.
122. Lim W, Bae H, Bazer FW, Song G. C-C motif chemokine ligand 23 abolishes ER stress- and LPS-induced reduction in proliferation of bovine endometrial epithelial cells. *J Cell Physiol.* 2018;233(4):3529-3539.
123. Pace AM, Faure M, Bourne HR. Gi2-mediated activation of the MAP kinase cascade. *Mol Biol Cell.* 1995;6(12):1685-1695.
124. Mochizuki N, Ohba Y, Kiyokawa E, et al. Activation of the ERK/MAPK pathway by an isoform of rap1GAP associated with G alpha(i). *Nature.* 1999;400(6747):891-894.
125. Denis-Henriot D, de Mazancourt P, Morot M, Giudicelli Y. Mutant alpha-subunit of the G protein G12 activates proliferation and inhibits differentiation of 3T3-F442A preadipocytes. *Endocrinology.* 1998;139(6):2892-2899.
126. Dombret H, Gardin C. An update of current treatments for adult acute myeloid leukemia. *Blood.* 2016;127(1):53-61.